

# Using $B_s^0 \rightarrow D_s^\mp K^\pm$ Decays as a Portal to New Physics

Robert Fleischer <sup>a,b</sup> and Eleftheria Malami <sup>a</sup>

<sup>a</sup>*Nikhef, Science Park 105, NL-1098 XG Amsterdam, Netherlands*

<sup>b</sup>*Department of Physics and Astronomy, Vrije Universiteit Amsterdam,  
NL-1081 HV Amsterdam, Netherlands*

## Abstract

The system of  $B_s^0 \rightarrow D_s^\mp K^\pm$  decays offers a theoretically clean determination of the angle  $\gamma$  of the Unitarity Triangle. A corresponding LHCb analysis resulted in a surprisingly large result, which is in tension with other determinations and global analyses of the Unitarity Triangle. Paying special attention to discrete ambiguities, we confirm this picture and resolve a final ambiguity. Moreover, we extract the branching ratios of the underlying  $\bar{B}_s^0 \rightarrow D_s^+ K^-$  and  $\bar{B}_s^0 \rightarrow D_s^- K^+$  modes. Combining them with information from semileptonic  $B_{(s)}$  decays, we arrive at another puzzling situation, which we obtain also for other decays with similar dynamics. These patterns could be footprints of New Physics in the  $b \rightarrow c\bar{u}s$  and  $b \rightarrow u\bar{c}s$  processes which govern the dynamics of the  $\bar{B}_s^0 \rightarrow D_s^\mp K^\pm$  channels. We present a model-independent strategy to reveal such effects. Applying it to the present data, we obtain strongly correlated New-Physics contributions with potentially large CP-violating phases. We find that new contributions sizeably smaller than the Standard Model amplitudes could actually accommodate the current data. This strategy offers an exciting probe for new sources of CP violation at the future high-precision frontier of  $B$  physics.



# 1 Introduction

The decays  $\bar{B}_s^0 \rightarrow D_s^+ K^-$  and  $B_s^0 \rightarrow D_s^+ K^-$  with their counterparts decaying into the CP-conjugate final state  $D_s^- K^+$  provide a particularly interesting laboratory for the exploration of CP violation [1–3]. In the Standard Model (SM), these channels originate only from tree-diagram-like topologies caused by  $b \rightarrow c\bar{u}s$  and  $\bar{b} \rightarrow \bar{u}c\bar{s}$  quark-level processes, respectively. Thanks to  $B_s^0\text{--}\bar{B}_s^0$  mixing, interference effects between the different decay paths into the  $D_s^\mp K^\pm$  final states arise, thereby providing observables which allow the determination of a CP-violating phase  $\phi_s + \gamma$ . Here  $\gamma$  is the usual angle of the Unitarity Triangle (UT), while  $\phi_s$  is the CP-violating  $B_s^0\text{--}\bar{B}_s^0$  mixing phase. The key feature of this method is that non-perturbative hadronic matrix elements of four-quark operators cancel in certain combinations of CP-violating observables, thereby resulting in a theoretically clean determination of  $\phi_s + \gamma$  within the SM. The value of  $\gamma$  can then be extracted with the help of the measured value of  $\phi_s$ , which can be determined through CP violation in  $B_s^0 \rightarrow J/\psi\phi$  decays and channels with similar dynamics [4–8].

The LHCb collaboration has performed an interesting study of CP violation in the system of the  $\bar{B}_s^0 \rightarrow D_s^\mp K^\pm$  and  $B_s^0 \rightarrow D_s^\mp K^\pm$  decays, reporting the result

$$\gamma = (128_{-22}^{+17})^\circ \quad (1)$$

modulo  $180^\circ$  from a fit to the data, where the uncertainty contains both statistical and systematic contributions [9]. Strategies utilising decays of the kind  $B \rightarrow DK$ , which also originate only from tree-level topologies in the SM, result in values of  $\gamma$  in the regime of  $70^\circ$  [10, 11], which is also consistent with global analyses of the UT [12, 13]. Consequently, despite the significant uncertainty, the result for  $\gamma$  in Eq. (1) with its central value much larger than  $70^\circ$  is intriguing. Could it actually indicate new sources of CP violation originating from physics beyond the SM? In order to shed light on this question, we will have an independent look at the extraction of  $\gamma$ , paying special attention to discrete ambiguities and their resolution [2, 3]. We obtain a picture fully consistent with Eq. (1), and resolve the final ambiguity of modulo  $180^\circ$ , corresponding to  $\gamma = (-52_{-22}^{+17})^\circ$ .

Further puzzling patterns arise in  $\bar{B}_d^0 \rightarrow D_d^+ K^-$ ,  $\bar{B}_d^0 \rightarrow D_d^+ \pi^-$  and  $\bar{B}_s^0 \rightarrow D_s^+ \pi^-$  modes, which are tree decays with dynamics similar to  $\bar{B}_s^0 \rightarrow D_s^+ K^-$ . Their branching ratios are found experimentally to be too small with respect to QCD factorisation [14, 15], which is expected to work very well in this decay class [16]. This feature has recently been addressed within New Physics (NP) analyses [17–19]; NP effects in non-leptonic tree-level decays of  $B$  mesons were also studied in Refs. [20, 21]. What is the corresponding situation for the branching ratios of the  $\bar{B}_s^0 \rightarrow D_s^+ K^-$  and  $B_s^0 \rightarrow D_s^+ K^-$  modes? We will extract these quantities from the experimental data. Complementing the branching ratios with information from semileptonic  $B_{(s)}$  decays, we determine parameters characterising factorisation from the data. For the  $\bar{B}_s^0 \rightarrow D_s^+ K^-$  channel, we obtain a picture similar to the  $\bar{B}_d^0 \rightarrow D_d^+ K^-$ ,  $\bar{B}_d^0 \rightarrow D_d^+ \pi^-$  and  $\bar{B}_s^0 \rightarrow D_s^+ \pi^-$  modes, showing tension with QCD factorisation as well. Interestingly, we find such a pattern – although with larger uncertainties – also for  $B_s^0 \rightarrow D_s^+ K^-$  and  $B_d^0 \rightarrow D_s^+ \pi^-$ , having similar dynamics.

In view of these puzzles in the data for the  $B_s^0 \rightarrow D_s^\mp K^\pm$  decays, we allow for CP-violating NP contributions and present a new strategy to reveal such effects. The corre-

sponding model-independent formalism allows a transparent analysis to constrain possible NP effects with potentially large CP-violating phases. We go beyond assumptions made in the LHCb analysis [9], point out SM relations and propose new measurements and aspects for future experimental studies.

In our analysis of the  $B_s^0 \rightarrow D_s^\mp K^\pm$  system, we first assume the SM. The outline of this paper is as follows: in Section 2, we have a closer look at CP violation and discuss the determination of  $\phi_s + \gamma$  from the measured observables, paying special attention to discrete ambiguities and their resolution. In Section 3, we extract the branching ratios of the individual  $B_s^0 \rightarrow D_s^+ K^-$  and  $B_s^0 \rightarrow D_s^- K^+$  channels from the experimental data. Complementing them with information from semileptonic  $B_{(s)}$  decays, we determine hadronic parameters, allowing a comparison with QCD factorisation. In view of the puzzling patterns arising in these studies, we extend the analysis to include contributions from physics beyond the SM in Section 4. Here we present a model-independent framework to reveal possible NP effects from the data, and apply it to the currently available measurements. Finally, we summarise our findings and conclusions in Section 5.

## 2 CP Violation

Since  $B_s^0$  and  $\bar{B}_s^0$  mesons may both decay into the same final state  $D_s^+ K^-$ , we obtain interference between the corresponding decay amplitudes through  $B_s^0$ - $\bar{B}_s^0$  mixing, which leads to time-dependent decay rates. In order to probe the corresponding CP-violating effects, rate asymmetries of the following kind are considered [2, 3]:

$$\frac{\Gamma(B_s^0(t) \rightarrow D_s^+ K^-) - \Gamma(\bar{B}_s^0(t) \rightarrow D_s^+ K^-)}{\Gamma(B_s^0(t) \rightarrow D_s^+ K^-) + \Gamma(\bar{B}_s^0(t) \rightarrow D_s^+ K^-)} = \frac{C \cos(\Delta M_s t) + S \sin(\Delta M_s t)}{\cosh(y_s t/\tau_{B_s}) + \mathcal{A}_{\Delta\Gamma} \sinh(y_s t/\tau_{B_s})}; \quad (2)$$

an analogous expression holds for the CP-conjugate final state  $D_s^- K^+$ , where  $C$ ,  $S$  and  $\mathcal{A}_{\Delta\Gamma}$  are replaced by  $\bar{C}$ ,  $\bar{S}$  and  $\bar{\mathcal{A}}_{\Delta\Gamma}$ , respectively. These observables satisfy the following sum rules:

$$\Delta_{\text{SR}} \equiv 1 - C^2 - S^2 - \mathcal{A}_{\Delta\Gamma}^2 = 0, \quad \bar{\Delta}_{\text{SR}} \equiv 1 - \bar{C}^2 - \bar{S}^2 - \bar{\mathcal{A}}_{\Delta\Gamma}^2 = 0. \quad (3)$$

In Eq. (2),  $\Delta M_s \equiv M_{\text{H}}^{(s)} - M_{\text{L}}^{(s)}$  describes the mass difference of the  $B_s$  mass eigenstates while their decay width difference  $\Delta\Gamma_s \equiv \Gamma_{\text{L}}^{(s)} - \Gamma_{\text{H}}^{(s)}$  enters the parameter

$$y_s \equiv \frac{\Delta\Gamma_s}{2\Gamma_s} = 0.062 \pm 0.004, \quad (4)$$

where  $\Gamma_s \equiv \tau_{B_s}^{-1}$  is the inverse of the average lifetime of the  $B_s$  system, and the numerical value corresponds to the current experimental average [11]. It should be noted that the decay width parameter  $y_s$  is sizeable in the  $B_s$  system, while its  $B_d$  counterpart takes a value at the per mille level. Thanks to this feature, we may get experimental access to the observable  $\mathcal{A}_{\Delta\Gamma}$  in  $B_s$  decays, as can be seen in Eq. (2).

The interference effects between  $B_s^0$ - $\bar{B}_s^0$  mixing and decay processes giving rise to the structure of Eq. (2) are described by the following observable [2]:

$$\xi = -e^{-i\phi_s} \left[ e^{i\phi_{\text{CP}}} \frac{A(\bar{B}_s^0 \rightarrow D_s^+ K^-)}{A(B_s^0 \rightarrow D_s^+ K^-)} \right], \quad (5)$$

where the decay amplitudes  $A(\bar{B}_s^0 \rightarrow D_s^+ K^-)$  and  $A(B_s^0 \rightarrow D_s^+ K^-)$  enter and  $\phi_s$  is the CP-violating  $B_s^0$ - $\bar{B}_s^0$  mixing phase. The latter quantity can be determined through CP-violating effects in  $B_s^0 \rightarrow J/\psi\phi$  and similar modes [4–8]. Using an average of the corresponding measurements and including corrections from doubly Cabibbo-suppressed penguin topologies through control channels yields

$$\phi_s = (-5_{-1.5}^{+1.6})^\circ, \quad (6)$$

while the SM prediction takes a value around  $-2^\circ$ , as discussed in detail in Ref. [8].

The convention-dependent phase  $\phi_{\text{CP}}$  in Eq. (5) is cancelled by the ratio of hadronic matrix elements, yielding

$$\xi = -e^{-i(\phi_s+\gamma)} \left[ \frac{1}{x_s e^{i\delta_s}} \right], \quad (7)$$

where  $x_s$  with the CP-conserving strong phase  $\delta_s$  parametrize the ratio of decay amplitudes, which depend on the corresponding hadronic matrix elements and elements of the Cabibbo–Kobayashi–Maskawa (CKM) matrix [2, 3]. The interference effects of the decays into the CP-conjugate final state  $D^- K^+$  are described by the observable

$$\bar{\xi} = -e^{-i(\phi_s+\gamma)} [x_s e^{i\delta_s}]. \quad (8)$$

We notice the following relation:

$$\xi \times \bar{\xi} = e^{-i2(\phi_s+\gamma)}, \quad (9)$$

where the non-perturbative parameter  $x_s e^{i\delta_s}$  cancels. Consequently, Eq. (9) is not affected by hadronic uncertainties, thereby representing a *theoretically clean* expression which offers access to the CP-violating phase  $\phi_s + \gamma$ . Using the value of  $\phi_s$  in Eq. (6), we may extract the UT angle  $\gamma$ .

The observables entering the time-dependent rate asymmetry in Eq. (2) are given in terms of  $\xi$  as follows:

$$C = \frac{1 - |\xi|^2}{1 + |\xi|^2}, \quad S = \frac{2 \text{Im } \xi}{1 + |\xi|^2}, \quad \mathcal{A}_{\Delta\Gamma} = \frac{2 \text{Re } \xi}{1 + |\xi|^2}. \quad (10)$$

Similar expressions hold for the CP-conjugate observables, where  $\xi$  is replaced by  $\bar{\xi}$ . Note that these expressions actually satisfy the sum rules in Eq. (3).

It should be emphasised that Eqs. (7) and (8) rely on the SM structure of the corresponding decay amplitudes, yielding

$$|\bar{\xi}| = \frac{1}{|\xi|}, \quad (11)$$

which implies

$$C + \bar{C} = 0. \quad (12)$$

In the analysis presented in Ref. [9], the LHCb collaboration has assumed these relations.

The absolute value of  $\xi$  can be determined from the measured value of  $C$  through

$$|\xi| = \sqrt{\frac{1-C}{1+C}}, \quad (13)$$

Observables	
$C = -0.73 \pm 0.15$	$\bar{C} = +0.73 \pm 0.15$
$S = +0.49 \pm 0.21$	$\bar{S} = +0.52 \pm 0.21$
$\mathcal{A}_{\Delta\Gamma} = +0.31 \pm 0.32$	$\bar{\mathcal{A}}_{\Delta\Gamma} = +0.39 \pm 0.32$
$\langle S \rangle_+ = 0.50 \pm 0.15$	$\langle S \rangle_- = 0.02 \pm 0.15$
$\langle \mathcal{A}_{\Delta\Gamma} \rangle_+ = 0.35 \pm 0.23$	$\langle \mathcal{A}_{\Delta\Gamma} \rangle_- = 0.04 \pm 0.23$

Table 1: CP-violating  $B_s^0 \rightarrow D_s^\mp K^\pm$  observables corresponding to the LHCb analysis in Ref. [9], with the observable combinations introduced in Eq. (16). Note that the results assume the relation in Eq. (12).

while further information from  $\mathcal{A}_{\Delta\Gamma}$  and  $S$  allows the extraction of the real and imaginary parts, respectively, with the help of the expressions

$$\text{Re } \xi = \frac{\mathcal{A}_{\Delta\Gamma}}{1+C}, \quad \text{Im } \xi = \frac{S}{1+C}, \quad (14)$$

thereby fixing the complex  $\xi$  from the data. In analogy, the observables corresponding to the CP-conjugate state  $D_s^- K^+$  allow us to determine  $\bar{\xi}$ . We may then use the relation in Eq. (9) to determine  $\phi_s + \gamma$  in a theoretically clean way. Due to the multiplicative factor of two associated with this phase, we obtain a twofold ambiguity, modulo  $180^\circ$ .

In case we have only measurements of  $C$  and  $S$  available, we would obtain a twofold ambiguity for  $\xi$ , and in analogy for  $\bar{\xi}$ . Consequently, we would then have a fourfold ambiguity for  $2(\phi_s + \gamma)$  when applying Eq. (9), resulting in an eightfold ambiguity for  $\phi_s + \gamma$ , and finally  $\gamma$  itself. However, due to the sizeable decay width difference  $\Delta\Gamma_s$ , we actually obtain access to the observables  $\mathcal{A}_{\Delta\Gamma}$  and  $\bar{\mathcal{A}}_{\Delta\Gamma}$ , thereby just leaving a twofold ambiguity, as was also pointed out in Refs. [2, 3].

Using the LHCb results reported in Ref. [9] and taking the proper sign conventions into account, we obtain the observables collected in Table 1, where we have added the statistical and systematic uncertainties in quadrature. It is interesting to observe that these measured values are consistent with the sum rules in Eq. (3):

$$\Delta_{\text{SR}} = 0.13 \pm 0.36, \quad \bar{\Delta}_{\text{SR}} = 0.04 \pm 0.40. \quad (15)$$

We give also the values for the combinations

$$\langle S \rangle_\pm \equiv \frac{\bar{S} \pm S}{2}, \quad \langle \mathcal{A}_{\Delta\Gamma} \rangle_\pm \equiv \frac{\bar{\mathcal{A}}_{\Delta\Gamma} \pm \mathcal{A}_{\Delta\Gamma}}{2}, \quad (16)$$

which will be useful below. Applying Eqs. (11) and (13), we obtain

$$|\xi| = 2.53_{-0.59}^{+1.43}, \quad |\bar{\xi}| = 0.40 \pm 0.13. \quad (17)$$

In order to determine  $\phi_s + \gamma$  and  $\delta_s$ , we may use the following relations [2, 3]:

$$\tan(\phi_s + \gamma) = -\frac{\langle S \rangle_+}{\langle \mathcal{A}_{\Delta\Gamma} \rangle_+} = -1.45_{-2.76}^{+0.73} \quad (18)$$

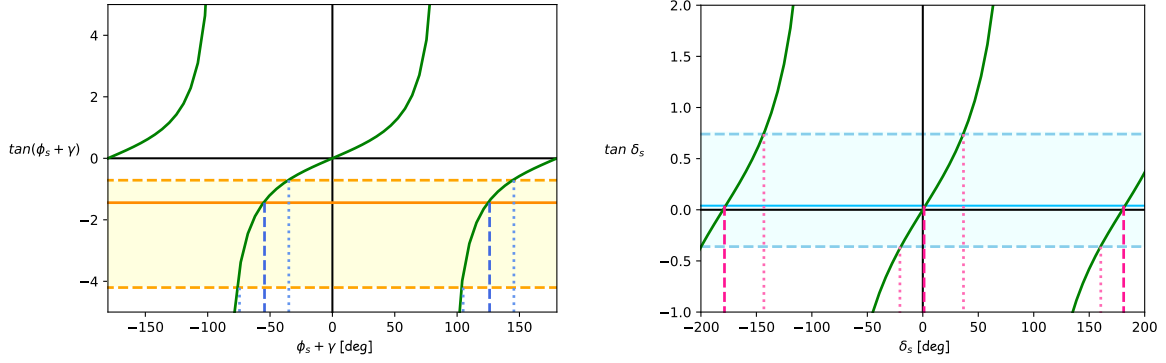


Figure 1: Illustration of  $\tan(\phi_s + \gamma)$  (left) and  $\tan \delta_s$  (right) with their experimental values as given in Eqs. (18) and (19), respectively.

$$\tan \delta_s = \frac{\langle S \rangle_-}{\langle \mathcal{A}_{\Delta\Gamma} \rangle_+} = 0.04_{-0.40}^{+0.70}, \quad (19)$$

which we have illustrated in Fig. 1. In the plot in the panel on the left-hand side, we can nicely see how the twofold solution for  $\phi_s + \gamma$  arises from the measured observables:

$$\phi_s + \gamma = (-55_{-18}^{+22})^\circ \quad \vee \quad (125_{-18}^{+22})^\circ. \quad (20)$$

Concerning the CP-conserving strong phase  $\delta_s$ , we obtain

$$\delta_s = (182_{-22}^{+34})^\circ \quad \vee \quad (2_{-22}^{+34})^\circ, \quad (21)$$

as illustrated in the plot in the panel on the right-hand side in Fig. 1. Using

$$\frac{\langle S \rangle_+}{\sqrt{1 - C^2}} = +\cos \delta_s \sin(\phi_s + \gamma), \quad \frac{\langle \mathcal{A}_{\Delta\Gamma} \rangle_+}{\sqrt{1 - C^2}} = -\cos \delta_s \cos(\phi_s + \gamma) \quad (22)$$

and taking the signs of  $\langle S \rangle_+$  and  $\langle \mathcal{A}_{\Delta\Gamma} \rangle_+$  in Table 1 into account, we observe that  $(\phi_s + \gamma) \sim -55^\circ$  and  $125^\circ$  are associated with  $\delta_s \sim 180^\circ$  and  $0^\circ$ , respectively. Note that  $\langle S \rangle_-$  and  $\langle \mathcal{A}_{\Delta\Gamma} \rangle_-$  are both proportional to  $\sin \delta_s$ , which is also reflected by their small experimental values. As pointed out in Ref. [2], the case of  $\delta_s \sim 0^\circ$  corresponds to the picture of factorisation, which we will discuss in more detail in Subsection 3.3. Consequently, this framework allows us to single out the solution  $(\phi_s + \gamma) \sim 125^\circ$  with  $\delta_s \sim 0^\circ$ , thereby excluding the values modulo  $180^\circ$ .

The LHCb collaboration has obtained results in Ref. [9] that are consistent with our findings in Eqs. (20) and (21). Performing a fit to the experimental data, taking also the relevant correlations into account, a sharper picture arises:

$$\phi_s + \gamma = (126_{-22}^{+17})^\circ, \quad \delta_s = (-2_{-14}^{+13})^\circ, \quad x_s = |\bar{\xi}| = 0.37_{-0.09}^{+0.10}. \quad (23)$$

Here we have used  $\phi_s = (-1.7 \pm 1.9)^\circ$  to convert the value of  $\gamma$  in Eq. (1) into  $\phi_s + \gamma$ , and have omitted the excluded solutions modulo  $180^\circ$ . Using the result for  $\phi_s$  in Eq. (6), which takes penguin corrections into account, we obtain

$$\gamma = (131_{-22}^{+17})^\circ. \quad (24)$$

The value for  $|\bar{\xi}|$  is consistent with the one in Eq. (17). In Refs. [2, 3], assuming the SM expressions for the relevant decay amplitudes, the hadronic parameters  $x_s$  and  $\delta_s$  were determined through data for  $B_d^0 \rightarrow D^\pm \pi^\mp$  decays, which are related to the  $B_s^0 \rightarrow D_s^\mp K^\pm$  system through the  $U$ -spin symmetry of strong interactions. These results are in good agreement with those in Eq. (23) within the uncertainties.

The result for  $\gamma$  in Eq. (24) with its central value much larger than the regime of  $70^\circ$ , which arises from analyses of pure tree-level decays of the kind  $B \rightarrow DK$  as well as from global fits of the UT, is intriguing despite its significant uncertainty. In order to shed more light on this puzzling situation, which could be due to NP effects entering the amplitudes of the  $B_s^0 \rightarrow D_s^\mp K^\pm$  decays, let us next have a closer look at the corresponding branching ratios.

### 3 Branching Ratios

#### 3.1 Disentangling the Branching Ratios

In the  $B_s^0 \rightarrow D_s^\mp K^\pm$  system, complications arise due to the interference between the different decay paths as well as the impact of  $B_s^0$ - $\bar{B}_s^0$  mixing. Let us first “switch off” the mixing effects and focus on disentangling the different decay contributions, considering  $\bar{B}_s^0$  and  $B_s^0$  decays into the final state  $D_s^+ K^-$ . We introduce the branching ratio

$$\mathcal{B}_{\text{th}} \equiv \frac{1}{2} [\mathcal{B}(\bar{B}_s^0 \rightarrow D_s^+ K^-)_{\text{th}} + \mathcal{B}(B_s^0 \rightarrow D_s^+ K^-)_{\text{th}}], \quad (25)$$

where the factor of one half arises from the average of the  $\bar{B}_s^0$  and  $B_s^0$  decays. The individual branching ratios

$$\mathcal{B}(\bar{B}_s^0 \rightarrow D_s^+ K^-)_{\text{th}} = |A(\bar{B}_s^0 \rightarrow D_s^+ K^-)|^2 \Phi_{\text{Ph}} \tau_{B_s} \quad (26)$$

$$\mathcal{B}(B_s^0 \rightarrow D_s^+ K^-)_{\text{th}} = |A(B_s^0 \rightarrow D_s^+ K^-)|^2 \Phi_{\text{Ph}} \tau_{B_s} \quad (27)$$

involve the corresponding decay amplitudes with the phase-space factor

$$\Phi_{\text{Ph}} \equiv \frac{1}{16 \pi m_{B_s}} \Phi \left( \frac{m_{D_s}}{m_{B_s}}, \frac{m_K}{m_{B_s}} \right), \quad (28)$$

where the meson masses  $m_{B_s}$ ,  $m_{D_s}$  and  $m_K$  enter the phase-space function

$$\Phi(x, y) \equiv \sqrt{[1 - (x + y)^2][1 - (x - y)^2]}. \quad (29)$$

The “theoretical” branching ratio (25) is related to the “experimental” branching ratio

$$\mathcal{B}_{\text{exp}} = \frac{1}{2} \int_0^\infty [\Gamma(\bar{B}_s^0(t) \rightarrow D_s^+ K^-) + \Gamma(B_s^0(t) \rightarrow D_s^+ K^-)] dt, \quad (30)$$

which corresponds to the time-integrated untagged decay rate [5], as follows [22]:

$$\mathcal{B}_{\text{th}} = \left[ \frac{1 - y_s^2}{1 + \mathcal{A}_{\Delta\Gamma_s} y_s} \right] \mathcal{B}_{\text{exp}}. \quad (31)$$



Using Eq. (5), we may write

$$\mathcal{B}_{\text{th}} = \frac{1}{2} (1 + |\xi|^2) \mathcal{B}_{\text{th}}(B_s^0 \rightarrow D_s^+ K^-) = \frac{1}{2} (1 + |\xi|^{-2}) \mathcal{B}_{\text{th}}(\bar{B}_s^0 \rightarrow D_s^+ K^-), \quad (32)$$

and obtain

$$\mathcal{B}(\bar{B}_s^0 \rightarrow D_s^+ K^-)_{\text{th}} = 2 \left( \frac{|\xi|^2}{1 + |\xi|^2} \right) \mathcal{B}_{\text{th}} \quad (33)$$

$$\mathcal{B}(B_s^0 \rightarrow D_s^+ K^-)_{\text{th}} = 2 \left( \frac{1}{1 + |\xi|^2} \right) \mathcal{B}_{\text{th}}, \quad (34)$$

where  $\mathcal{B}_{\text{th}}$  can be determined from the experimental branching ratio through Eq. (31).

For the  $\bar{B}_s^0$  and  $B_s^0$  decays into the CP-conjugate final state  $D_s^- K^+$ , we obtain analogous expressions, where we have to replace  $\mathcal{B}_{\text{exp}}$ ,  $\mathcal{B}_{\text{theo}}$ ,  $\mathcal{A}_{\Delta\Gamma_s}$  and  $\xi$  through their counterparts  $\bar{\mathcal{B}}_{\text{exp}}$ ,  $\bar{\mathcal{B}}_{\text{theo}}$ ,  $\bar{\mathcal{A}}_{\Delta\Gamma_s}$  and  $\bar{\xi}$ , respectively. In analogy to Eqs. (33) and (34), we may then also determine the theoretical branching ratios of the  $\bar{B}_s^0 \rightarrow D_s^- K^+$  and  $B_s^0 \rightarrow D_s^- K^+$  modes. In the SM, we have the following relations:

$$\mathcal{B}(\bar{B}_s^0 \rightarrow D_s^- K^+)_{\text{th}} \stackrel{\text{SM}}{=} \mathcal{B}(B_s^0 \rightarrow D_s^- K^+)_{\text{th}} \quad (35)$$

$$\mathcal{B}(B_s^0 \rightarrow D_s^+ K^-)_{\text{th}} \stackrel{\text{SM}}{=} \mathcal{B}(\bar{B}_s^0 \rightarrow D_s^- K^+)_{\text{th}}, \quad (36)$$

yielding

$$\mathcal{B}_{\text{th}} \stackrel{\text{SM}}{=} \bar{\mathcal{B}}_{\text{th}}. \quad (37)$$

It would be very interesting to test these SM relations through separate measurements of the experimental branching ratios  $\mathcal{B}_{\text{exp}}$  and  $\bar{\mathcal{B}}_{\text{exp}}$ . Unfortunately, such results have not yet been reported. However, there are measurements of the following average [11]:

$$\mathcal{B}_{\Sigma}^{\text{exp}} \equiv \mathcal{B}_{\text{exp}} + \bar{\mathcal{B}}_{\text{exp}} = (2.27 \pm 0.19) \times 10^{-4}. \quad (38)$$

Assuming now, as was also done by the LHCb collaboration [9], again the framework of the SM, we obtain the following relation [3]:

$$\mathcal{B}_{\text{th}} = \bar{\mathcal{B}}_{\text{th}} = \left[ \frac{1 - y_s^2}{1 + y_s \langle \mathcal{A}_{\Delta\Gamma} \rangle_+} \right] \langle \mathcal{B}_{\text{exp}} \rangle, \quad (39)$$

where  $\langle \mathcal{A}_{\Delta\Gamma} \rangle_+$  was introduced in Eq. (16), and

$$\langle \mathcal{B}_{\text{exp}} \rangle \equiv \frac{1}{2} (\mathcal{B}_{\text{exp}} + \bar{\mathcal{B}}_{\text{exp}}) = \frac{1}{2} \mathcal{B}_{\Sigma}^{\text{exp}}. \quad (40)$$

Parameters	Values
$\mathcal{B}_{\text{th}}$	$(1.10 \pm 0.09) \times 10^{-4}$
$\mathcal{B}(\bar{B}_s^0 \rightarrow D_s^+ K^-)_{\text{th}}$	$(1.94 \pm 0.21) \times 10^{-4}$
$\mathcal{B}(B_s^0 \rightarrow D_s^+ K^-)_{\text{th}}$	$(0.26 \pm 0.12) \times 10^{-4}$

Table 2: Values of the theoretical branching ratios characterising the  $B_s^0 \rightarrow D_s^\mp K^\pm$  system, assuming vanishing NP contributions to the corresponding decay amplitudes, as discussed in the text.

Using then Eqs. (33) and (34) and the value of  $|\xi|$  extracted from the experimental study of CP violation discussed in Section 2, we may determine the theoretical branching ratios of the  $\bar{B}_s^0 \rightarrow D_s^+ K^-$  and  $B_s^0 \rightarrow D_s^+ K^-$  decays, which are – due to our assumption of the SM – equal to their CP conjugates. In Table 2, we summarise the corresponding results following from the current data.

### 3.2 Consistency of the Branching Ratios with Partner Decays and First Information on Exchange Topologies

It is instructive to compare the results collected in Table 2 with the branching ratios of the  $\bar{B}_d^0 \rightarrow D_d^+ K^-$  and  $B_d^0 \rightarrow D_s^+ \pi^-$  decays, which differ from the  $\bar{B}_s^0 \rightarrow D_s^+ K^-$  and  $B_s^0 \rightarrow D_s^+ K^-$  modes, respectively, only through their spectator quarks and originate from the same quark-level processes. The current experimental results, which are actually CP-averaged branching ratios, read as follows [11]:

$$\mathcal{B}(\bar{B}_d^0 \rightarrow D_d^+ K^-) = (1.86 \pm 0.20) \times 10^{-4}, \quad \mathcal{B}(B_d^0 \rightarrow D_s^+ \pi^-) = (2.16 \pm 0.26) \times 10^{-5}. \quad (41)$$

In contrast to their  $B_s$  counterparts, these modes do not receive contributions from exchange topologies. We may use the branching ratios to determine the ratios

$$\left| \frac{T_{D_s K}}{T_{D_d K}} \right|^2 \left| 1 + \frac{E_{D_s K}}{T_{D_s K}} \right|^2 = \frac{\tau_{B_d} m_{B_s}}{\tau_{B_s} m_{B_d}} \left[ \frac{\Phi(m_{D_d}/m_{B_d}, m_K/m_{B_d})}{\Phi(m_{D_s}/m_{B_s}, m_K/m_{B_s})} \right] \left[ \frac{\mathcal{B}(\bar{B}_s^0 \rightarrow D_s^+ K^-)_{\text{th}}}{\mathcal{B}(\bar{B}_d^0 \rightarrow D_d^+ K^-)} \right] \quad (42)$$

$$\left| \frac{T_{KD_s}}{T_{\pi D_s}} \right|^2 \left| 1 + \frac{E_{KD_s}}{T_{KD_s}} \right|^2 = \frac{\tau_{B_d} m_{B_s}}{\tau_{B_s} m_{B_d}} \left[ \frac{\Phi(m_{D_s}/m_{B_d}, m_\pi/m_{B_d})}{\Phi(m_{D_s}/m_{B_s}, m_K/m_{B_s})} \right] \left[ \frac{\mathcal{B}(B_s^0 \rightarrow D_s^+ K^-)_{\text{th}}}{\mathcal{B}(B_d^0 \rightarrow D_s^+ \pi^-)} \right], \quad (43)$$

where the  $E$  and  $T$  amplitudes describe the corresponding exchange and colour-allowed tree topologies. The  $SU(3)$  flavour symmetry of strong interactions implies

$$T_{D_s K} \approx T_{D_d K}, \quad T_{KD_s} \approx T_{\pi D_s}, \quad (44)$$

where  $SU(3)$ -breaking corrections may only arise from the spectator quarks. Using the experimental results in Table 2 and Eq. (41) with the meson masses in Table 3 and the following values of the average lifetimes of the  $B_s^0$  and  $B_d^0$  mesons [11]:

$$\tau_{B_s} = (1.527 \pm 0.011) \text{ ps}, \quad \tau_{B_d} = (1.519 \pm 0.004) \text{ ps}, \quad (45)$$

we obtain

$$\left| \frac{T_{D_s K}}{T_{D_d K}} \right| \left| 1 + \frac{E_{D_s K}}{T_{D_s K}} \right| = 1.03 \pm 0.08 \quad (46)$$

$$\left| \frac{T_{KD_s}}{T_{\pi D_s}} \right| \left| 1 + \frac{E_{KD_s}}{T_{KD_s}} \right| = 1.11 \pm 0.26. \quad (47)$$

These findings are consistent with a smallish impact of the exchange topologies, which was also found in Refs. [3, 14]. We shall quantify this picture in more detail in our analysis in Subsection 3.3.

Masses	Values
$m_{B_s}$	$(5366.88 \pm 0.14)$ MeV
$m_{B_d}$	$(5279.64 \pm 0.12)$ MeV
$m_{D_s}$	$(1968.34 \pm 0.07)$ MeV
$m_{D_d}$	$(1869.66 \pm 0.05)$ MeV
$m_K$	$(493.677 \pm 0.016)$ MeV
$m_\pi$	$(139.5704 \pm 0.0002)$ MeV

Table 3: Meson masses relevant for our numerical analysis [11].

The decays  $\bar{B}_d^0 \rightarrow D_d^+ \pi^-$  and  $\bar{B}_s^0 \rightarrow D_s^+ \pi^-$  originate from  $b \rightarrow \bar{c}ud$  quark-level processes and are related to the  $\bar{B}_s^0 \rightarrow D_s^+ K^-$  and  $\bar{B}_d^0 \rightarrow D_d^+ K^-$  modes through the  $U$ -spin symmetry of strong interactions, respectively [2, 3], allowing us to determine

$$\left| \frac{T_{D_d \pi}}{T_{D_s \pi}} \right|^2 \left| 1 + \frac{E_{D_d \pi}}{T_{D_d \pi}} \right|^2 = \frac{\tau_{B_s} m_{B_d}}{\tau_{B_d} m_{B_s}} \left[ \frac{\Phi(m_{D_s}/m_{B_s}, m_\pi/m_{B_s})}{\Phi(m_{D_d}/m_{B_d}, m_\pi/m_{B_d})} \right] \left[ \frac{\mathcal{B}(\bar{B}_d^0 \rightarrow D_d^+ \pi^-)}{\mathcal{B}(\bar{B}_s^0 \rightarrow D_s^+ \pi^-)_{\text{th}}} \right]. \quad (48)$$

Using the relation

$$\mathcal{B}(\bar{B}_s^0 \rightarrow D_s^+ \pi^-)_{\text{th}} = (1 - y_s^2) \mathcal{B}(\bar{B}_s^0 \rightarrow D_s^+ \pi^-)_{\text{exp}} \quad (49)$$

between the theoretical and experimental  $\bar{B}_s^0 \rightarrow D_s^+ \pi^-$  branching ratios [22], and the following experimental results [11]

$$\mathcal{B}(\bar{B}_d^0 \rightarrow D_d^+ \pi^-) = (2.52 \pm 0.13) \times 10^{-3}, \quad \mathcal{B}(\bar{B}_s^0 \rightarrow D_s^+ \pi^-)_{\text{exp}} = (3.00 \pm 0.23) \times 10^{-3}, \quad (50)$$

we obtain

$$\left| \frac{T_{D_d \pi}}{T_{D_s \pi}} \right| \left| 1 + \frac{E_{D_d \pi}}{T_{D_d \pi}} \right| = 0.91 \pm 0.04, \quad (51)$$

which is consistent with Eq. (46) within the uncertainties.

### 3.3 Factorisation

The calculation of non-leptonic  $B$ -meson decays is challenging due to the impact of strong interactions. Since decades, the ‘‘factorisation’’ approach is applied as a particularly useful tool, where the hadronic matrix elements of the corresponding four-quark operators are factorised into the matrix elements of their quark currents. Factorisation is not a universal feature of non-leptonic  $B$  decays. Key examples where it is expected to work very well is given by decays of the kind  $\bar{B}_s^0 \rightarrow D_s^+ \pi^-$  and  $\bar{B}_d^0 \rightarrow D_d^+ K^-$ , which originate only from colour-allowed tree-diagram-like topologies [16, 23–26].

The  $\bar{B}_s^0 \rightarrow D_s^+ K^-$  channel, which plays a key role for our analysis, differs from  $\bar{B}_d^0 \rightarrow D_d^+ K^-$  only through the spectator quark and is also caused by  $b \rightarrow \bar{c}us$  quark-level transitions. As we have seen above, it receives an additional contribution from an exchange topology, which involves the spectator quark and does not factorise. However, experimental data show that such exchange topologies contribute to the decay amplitudes at the few-percent level [14], thereby playing a minor role. In Eq. (46), we have obtained a result consistent with these findings, which are actually also theoretically expected [14].

Within the SM, we may write the  $\bar{B}_s^0 \rightarrow D_s^+ K^-$  decay amplitude as follows:

$$A_{\bar{B}_s^0 \rightarrow D_s^+ K^-}^{\text{SM}} = \frac{G_F}{\sqrt{2}} V_{us}^* V_{cb} f_K F_0^{B_s \rightarrow D_s}(m_K^2) (m_{B_s}^2 - m_{D_s}^2) a_{1\text{eff}}^{D_s K}, \quad (52)$$

where  $G_F$  is the Fermi constant,  $V_{us}^* V_{cb}$  contains the relevant CKM matrix elements,  $f_K$  is the kaon decay constant, and  $F_0^{B_s \rightarrow D_s}(m_K^2)$  is a form factor entering the parametrisation of the hadronic  $b \rightarrow c$  quark-current matrix element:

$$\begin{aligned} \langle D_s^+(k) | \bar{c} \gamma_\mu b | \bar{B}_s^0(p) \rangle &= \\ &= F_0(q^2) \left( \frac{m_{B_s}^2 - m_{D_s}^2}{q^2} \right) q_\mu + F_1(q^2) \left[ (p+k)_\mu - \left( \frac{m_{B_s}^2 - m_{D_s}^2}{q^2} \right) q_\mu \right], \end{aligned} \quad (53)$$

where  $q \equiv p - k$  denotes the four-momentum transfer. The form factors can be calculated with a variety of approaches, most notably lattice QCD [27–29]. The parameter

$$a_{1\text{eff}}^{D_s K} = a_1^{D_s K} \left( 1 + \frac{E_{D_s K}}{T_{D_s K}} \right) \quad (54)$$

describes the deviation from naive factorisation. Here  $a_1^{D_s K}$  characterises the non-factorisable effects entering the colour-allowed tree amplitude  $T_{D_s K}$ , while  $E_{D_s K}$  describes the non-factorisable exchange topologies, as introduced in Eq. (42).

In the analysis within the QCD factorisation approach in Ref. [16], the  $a_1$  parameters for colour-allowed  $\bar{B} \rightarrow DP$  decays ( $P = \pi, K$ ) originating from  $b \rightarrow \bar{c}ur$  quark-level transitions ( $r = d, s$ ) are found as  $|a_1| \approx 1.05$  with a quasi-universal behaviour, which illustrates that factorisation is expected to work very well in this decay class. Another indication of this feature comes from the stable behaviour of  $a_1$  under the QCD renormalisation group evolution [30, 31], which is in contrast to the  $a_2$  coefficient characterising colour-suppressed decays, where factorisation is not expected to work well. Interestingly, for decays of the kind  $\bar{B}_d^0 \rightarrow J/\psi \pi^0$ , experimental data give values for  $a_2(\bar{B}_d^0 \rightarrow J/\psi \pi^0)$  that are surprisingly consistent with the picture of naive factorisation [8].

The current state-of-the-art results for the decays  $\bar{B}_d^0 \rightarrow D_d^+ K^-$ ,  $\bar{B}_d^0 \rightarrow D_d^+ \pi^-$  and  $\bar{B}_s^0 \rightarrow D_s^+ \pi^-$  calculated in QCD factorisation are given as follows [15, 32]:

$$|a_1^{D_d K}| = 1.0702_{-0.0128}^{+0.0101}, \quad |a_1^{D_d \pi}| = 1.073_{-0.014}^{+0.012}, \quad |a_1^{D_s \pi}| = 1.0727_{-0.0140}^{+0.0125}. \quad (55)$$

These modes are related to one another through the  $SU(3)$  flavour symmetry of strong interactions, leading to an essentially negligible difference of their  $|a_1|$  parameters. We observe here also the quasi-universal behaviour noted above. Since the  $\bar{B}_s^0 \rightarrow D_s^+ K^-$  mode differs from the  $\bar{B}_d^0 \rightarrow D^+ K^-$  channel only through the spectator quarks, we may identify their  $|a_1|$  parameters and shall use

$$|a_1^{D_s K}| = 1.07 \pm 0.02, \quad (56)$$

where we have doubled the tiny error in view of  $SU(3)$ -breaking effects in the spectator quarks, taking the spread of the  $SU(3)$ -related values in Eq. (55) into account.

We may now calculate the ratios of the colour-allowed tree amplitudes entering the expressions in Eqs. (46) and (51):

$$\left| \frac{T_{D_s K}}{T_{D_d K}} \right| = \left[ \frac{F_0^{B_s \rightarrow D_s}(m_K^2)}{F_0^{B_d \rightarrow D_d}(m_K^2)} \right] \left[ \frac{m_{B_s}^2 - m_{D_s}^2}{m_{B_d}^2 - m_{D_d}^2} \right] \left| \frac{a_1^{D_s K}}{a_1^{D_d K}} \right| = 1.03 \pm 0.03 \quad (57)$$

$$\left| \frac{T_{D_d \pi}}{T_{D_s \pi}} \right| = \left[ \frac{F_0^{B_d \rightarrow D_d}(m_\pi^2)}{F_0^{B_s \rightarrow D_s}(m_\pi^2)} \right] \left[ \frac{m_{B_d}^2 - m_{D_d}^2}{m_{B_s}^2 - m_{D_s}^2} \right] \left| \frac{a_1^{D_\pi}}{a_1^{D_s \pi}} \right| = 0.99 \pm 0.03, \quad (58)$$

where we have used the following form-factor ratios [33]:

$$\left| \frac{F_0^{B_s \rightarrow D_s}(m_\pi^2)}{F_0^{B_d \rightarrow D_d}(m_\pi^2)} \right| = 1.01 \pm 0.02, \quad \left| \frac{F_0^{B_s \rightarrow D_s}(m_K^2)}{F_0^{B_d \rightarrow D_d}(m_K^2)} \right| = 1.01 \pm 0.02. \quad (59)$$

Finally, we obtain

$$r_E^{D_s K} \equiv \left| 1 + \frac{E_{D_s K}}{T_{D_s K}} \right| = 1.00 \pm 0.08, \quad r_E^{D_d \pi} \equiv \left| 1 + \frac{E_{D_d \pi}}{T_{D_d \pi}} \right| = 0.92 \pm 0.05. \quad (60)$$

These current state-of-the-art results do not indicate any anomalous behaviour of the exchange topologies, and are consistent with those obtained in Refs. [3, 14]. The strong constraints in Eq. (60) suggest a large strong phase difference between the exchange and colour-allowed tree amplitudes that may be generated through the non-factorisable contributions to the exchange topologies. Such a feature was also noted for similar amplitudes of other modes in Refs. [3, 14].

Let us now have a look at the  $B_s^0 \rightarrow K^+ D_s^-$  decay, which originates from  $b \rightarrow u \bar{c} s$  quark-level transitions. In the SM, we may write the decay amplitude – in analogy to Eq. (52) – in the form

$$A_{B_s^0 \rightarrow K^+ D_s^-}^{\text{SM}} = \frac{G_F}{\sqrt{2}} V_{cs}^* V_{ub} f_{D_s} F_0^{B_s \rightarrow K}(m_{D_s}^2) (m_{B_s}^2 - m_K^2) a_{1\text{eff}}^{KD_s} \quad (61)$$

with

$$a_{1\text{eff}}^{KD_s} = a_1^{KD_s} \left( 1 + \frac{E_{KD_s}}{T_{KD_s}} \right), \quad (62)$$

where the CKM factors are replaced correspondingly,  $f_{D_s}$  is the  $D_s$  decay constant, and  $F_0^{B_s \rightarrow K}(m_{D_s}^2)$  parametrises the hadronic matrix element of the  $b \rightarrow u$  transition. The coefficient  $a_1^{KD_s}$  describes non-factorisable contributions to the colour-allowed tree amplitude  $T_{KD_s}$ , while the amplitude  $E_{KD_s}$  arises from non-factorisable exchange topologies, as in Eq. (54). Although this channel is also colour-allowed, the heavy-quark arguments for QCD factorisation for the  $b \rightarrow c$  tree-level decays not apply in this case [16]. Consequently, we may expect larger non-factorisable effects in this case. As a reference point, using Eq. (56) as guidance, we assume the following value:

$$|a_1^{KD_s}| = 1.1 \pm 0.1, \quad (63)$$

where the uncertainty is five times larger than in (56). It would be interesting to have a dedicated theoretical study for this parameter, which is beyond the scope of this paper.

Interestingly, the strong phase difference  $\delta_s$  in Eq. (23), with a central value close to  $0^\circ$ , disfavours large non-factorisable long-distance effects entering through the  $\bar{B}_s^0 \rightarrow K^+ D_s^-$  decay path.

The amplitude of the decay  $\bar{B}_d^0 \rightarrow \pi^+ D_s^-$  takes the same form as Eq. (61). However, this channel does not have contributions from exchange topologies, thereby yielding

$$a_{1\text{eff}}^{\pi D_s} = a_1^{\pi D_s}. \quad (64)$$

We assume the relation

$$|a_1^{\pi D_s}| = |a_1^{K D_s}| = 1.1 \pm 0.1 \quad (65)$$

with the numerical value in Eq. (63). Applying the formulae given above yields

$$\left| \frac{T_{K D_s}}{T_{\pi D_s}} \right| = \left[ \frac{F_0^{B_s \rightarrow K}(m_{D_s}^2)}{F_0^{B_d \rightarrow \pi}(m_{D_s}^2)} \right] \left[ \frac{m_{B_s}^2 - m_K^2}{m_{B_d}^2 - m_\pi^2} \right] \left| \frac{a_1^{K D_s}}{a_1^{\pi D_s}} \right|. \quad (66)$$

The  $SU(3)$ -breaking form-factor ratio was calculated in Ref. [34], with the result

$$\left[ \frac{F_0^{B_s \rightarrow K}(m_{D_s}^2)}{F_0^{B_d \rightarrow \pi}(m_{D_s}^2)} \right] = 1.12 \pm 0.11. \quad (67)$$

Finally, employing Eq. (65) and the meson masses in Table 3, we find

$$\left| \frac{T_{K D_s}}{T_{\pi D_s}} \right| = 1.15 \pm 0.19, \quad (68)$$

which allows us to extract

$$r_E^{K D_s} \equiv \left| 1 + \frac{E_{K D_s}}{T_{K D_s}} \right| = 0.97 \pm 0.17 \quad (69)$$

from the numerical result in Eq. (47) following from the experimental data. We observe a pattern similar to the constraints in Eq. (60), although with larger uncertainty.

We would like to extract the  $|a_1|$  parameters of the  $\bar{B}_s^0 \rightarrow D_s^+ K^-$  and  $\bar{B}_s^0 \rightarrow K^+ D_s^-$  channels from the data in the cleanest possible way, comparing them with the theoretical expectations. The central question is whether we will again encounter a puzzling situation as in Section 2. In this respect, semileptonic decays provide a very useful tool.

## 3.4 Information from Semileptonic Decays

### 3.4.1 Preliminaries

Using expressions (25)–(29) and the decay amplitudes in Eqs. (52) and (61), we may calculate the corresponding “theoretical” branching ratios. These SM predictions require information on the CKM matrix elements  $|V_{cb}|$  and  $|V_{ub}|$  [35], as well as on the relevant non-perturbative hadronic form factors. In view of this feature, it is advantageous to combine these branching ratios with information from semileptonic  $B$  decays.

The differential rate of a semileptonic  $B \rightarrow P\ell\bar{\nu}_\ell$  decay, where  $P$  denotes a pseudoscalar meson, can be written in the following form (neglecting lepton masses) [36–39]:

$$\frac{d\Gamma(\bar{B} \rightarrow P\ell\bar{\nu}_\ell)}{dq^2} = \frac{G_F^2 |V_{rb}|^2}{192\pi^3} \left[ m_B \Phi \left( \frac{m_P}{m_B}, \frac{\sqrt{q^2}}{m_B} \right) \right]^3 [F_1^{B \rightarrow P}(q^2)]^2. \quad (70)$$

Here the label  $r = c, u$  distinguishes between  $b \rightarrow c\ell\bar{\nu}_\ell$  and  $b \rightarrow u\ell\bar{\nu}_\ell$  quark-level transitions, the phase-space function  $\Phi(x, y)$  was introduced in Eq. (29), and  $F_1^{B \rightarrow P}(q^2)$  is the second form factor parametrising the corresponding quark-current matrix element (see Eq. (53)), satisfying the normalisation condition

$$F_1^{B \rightarrow P}(0) = F_0^{B \rightarrow P}(0). \quad (71)$$

In Eq. (70), we have again assumed the SM for the semileptonic decay amplitude. The corresponding modes may be affected by physics from beyond the SM [40–43]. For strategies to constrain and include NP effects in such decays, see Refs. [44, 45] and references therein. Should physics beyond the SM enter exclusively through couplings to heavy tau leptons, which is a popular scenario in the literature, the semileptonic decay rates into muons and electrons would still take the form in Eq. (70). When using experimental data, we shall only employ semileptonic  $B_{(s)}$  decays into the light leptons  $\ell = e, \mu$  (and hence neglected the lepton masses in Eq. (70)).

### 3.4.2 System of the $\bar{B}_s^0 \rightarrow D_s^+ K^-$ and $\bar{B}_s^0 \rightarrow D_s^+ \ell \bar{\nu}_\ell$ Decays

Let us first have a look at the  $\bar{B}_s^0 \rightarrow D_s^+ K^-$  channel, which originates from a  $b \rightarrow c$  transition and is complemented through the semileptonic decay  $\bar{B}_s^0 \rightarrow D_s^+ \ell \bar{\nu}_\ell$ . It is very useful to introduce a ratio of the following kind [14, 16, 25]:

$$R_{D_s^+ K^-} \equiv \frac{\mathcal{B}(\bar{B}_s^0 \rightarrow D_s^+ K^-)_{\text{th}}}{d\mathcal{B}(\bar{B}_s^0 \rightarrow D_s^+ \ell \bar{\nu}_\ell) / dq^2 |_{q^2=m_K^2}}, \quad (72)$$

where the differential branching ratio

$$\frac{d\mathcal{B}(\bar{B}_s^0 \rightarrow D_s^+ \ell \bar{\nu}_\ell)}{dq^2} = \tau_{B_s} \left[ \frac{d\Gamma(\bar{B}_s^0 \rightarrow D_s^+ \ell \bar{\nu}_\ell)}{dq^2} \right] \quad (73)$$

is related to the differential rate through the  $B_s$  average lifetime  $\tau_{B_s}$ . It should be noted that for  $q^2 = m_K^2$ , the same phase space-functions enter the semileptonic and non-leptonic  $\bar{B}_s^0$  decays, and that the CKM matrix element  $|V_{cb}|$  cancels in the  $R_{D_s^+ K^-}$  ratio. Using Eqs. (26)–(29) with (70) and (73), we obtain

$$R_{D_s^+ K^-} = 6\pi^2 f_K^2 |V_{us}|^2 |a_{1\text{eff}}^{D_s K}|^2 X_{D_s K}, \quad (74)$$

where

$$X_{D_s K} = \frac{(m_{B_s}^2 - m_{D_s}^2)^2}{[m_{B_s}^2 - (m_{D_s} + m_K)^2][m_{B_s}^2 - (m_{D_s} - m_K)^2]} \left[ \frac{F_0^{B_s \rightarrow D_s}(m_K^2)}{F_1^{B_s \rightarrow D_s}(m_K^2)} \right]^2. \quad (75)$$

The product of the kaon decay constant and the CKM factor  $|V_{us}|$  can be extracted from data for leptonic  $K$  decays, yielding  $f_K|V_{us}| = (35.09 \pm 0.04 \pm 0.04) \text{ MeV}$  [46]. In Table 3, we collect the relevant meson masses. For the momentum transfer  $q^2 = m_K^2$ , the ratio of hadronic form factors is close to the normalisation given in Eq. (71). Using the form-factor information from lattice QCD studies [27–29], we obtain

$$\left[ \frac{F_0^{B_s \rightarrow D_s}(m_K^2)}{F_1^{B_s \rightarrow D_s}(m_K^2)} \right] = 1.00 \pm 0.03. \quad (76)$$

The differential rate of the  $\bar{B}_s^0 \rightarrow D_s^+ \ell^- \bar{\nu}_\ell$  decay has recently been measured by the LHCb collaboration [47]. Applying the Caprini–Lellouch–Neubert (CLN) parametrisation [48] of the relevant form factor with the parameters

$$|V_{cb}| = (41.4 \pm 1.3) \times 10^{-3}, \quad G(0) = 1.102 \pm 0.034, \quad \rho^2 = 1.27 \pm 0.05, \quad (77)$$

which result from the LHCb analysis [47], we obtain

$$\left. \frac{d\mathcal{B}(\bar{B}_s^0 \rightarrow D_s^+ \ell^- \bar{\nu}_\ell)}{dq^2} \right|_{q^2=m_K^2} = (3.97 \pm 0.47) \times 10^{-3} \text{ GeV}^{-2}, \quad (78)$$

where we have used Eq. (73) with the value of  $\tau_{B_s}$  in Eq. (45) to convert the differential rate into the differential branching ratio. Combining this result with the theoretical branching ratio for the  $\bar{B}_s^0 \rightarrow D_s^+ K^-$  mode in Table 2 yields

$$R_{D_s^+ K^-} = 0.05 \pm 0.01, \quad (79)$$

which allows us finally to determine

$$|a_{1\text{eff}}^{D_s K}| = 0.82 \pm 0.09. \quad (80)$$

Using the expression in (54) with

$$r_E^{D_s K} = 1.00 \pm 0.08 \quad (81)$$

given in Eq. (60) to take the contribution from the exchange topology into account, we obtain

$$|a_1^{D_s K}| = 0.82 \pm 0.11. \quad (82)$$

This result, which follows from the data and has a tiny dependence on hadronic form factors, has a surprisingly small central value and differs from the theoretical expectation in Eq. (56) at the  $2.2\sigma$  level. We shall return to this puzzling feature in Subsection 3.5.

### 3.4.3 System of the $\bar{B}_s^0 \rightarrow K^+ D_s^-$ and $\bar{B}_s^0 \rightarrow K^+ \ell^- \bar{\nu}_\ell$ Decays

The decay  $\bar{B}_s^0 \rightarrow K^+ D_s^-$  originates from a  $b \rightarrow u$  transition and is complemented through the semi-leptonic  $\bar{B}_s^0 \rightarrow K^+ \ell^- \bar{\nu}_\ell$  decay. In analogy to Eq. (72), we introduce the ratio

$$R_{K^+ D_s^-} \equiv \frac{\mathcal{B}(\bar{B}_s^0 \rightarrow D_s^- K^+)_{\text{th}}}{d\mathcal{B}(\bar{B}_s^0 \rightarrow K^+ \ell^- \bar{\nu}_\ell)/dq^2|_{q^2=m_{D_s}^2}}, \quad (83)$$



which takes the following form similar to Eq. (74):

$$R_{K^+D_s^-} = 6\pi^2 f_{D_s}^2 |V_{cs}|^2 |a_{1\text{eff}}^{KD_s}|^2 X_{KD_s}, \quad (84)$$

where

$$X_{KD_s} = \frac{(m_{B_s}^2 - m_K^2)^2}{[m_{B_s}^2 - (m_K + m_{D_s})^2][m_{B_s}^2 - (m_K - m_{D_s})^2]} \left[ \frac{F_0^{B_s \rightarrow K}(m_{D_s}^2)}{F_1^{B_s \rightarrow K}(m_{D_s}^2)} \right]^2. \quad (85)$$

The product of the  $D_s$  decay constant and the CKM factor  $|V_{cs}|$  can be determined from measurements of leptonic  $D_s$  decays, yielding  $f_{D_s}|V_{cs}| = (250.9 \pm 4.0)$  MeV [46].

The semileptonic  $\bar{B}_s^0 \rightarrow K^+ \ell \bar{\nu}_\ell$  mode, which would also be very useful for an analysis of the  $\bar{B}_s^0 \rightarrow K^+ K^-$  decay [49], has recently been observed by the LHCb collaboration with a first measurement of its branching ratio [50]. However, the corresponding differential decay rate for various  $q^2$  bins was not reported. Consequently, we may not yet determine the  $R_{K^+D_s^-}$  ratio from the data. However, applying the  $SU(3)$  flavour symmetry of strong interactions, we may replace the semileptonic  $B_s$  decay through its partner channel  $B_d^0 \rightarrow \pi^+ \ell^- \bar{\nu}_\ell$ , for which we do have measurements of the differential rate by the BaBar and Belle collaborations [10, 11]. We introduce

$$R_{K^+D_s^-}^{SU(3)} \equiv \frac{\mathcal{B}(\bar{B}_s^0 \rightarrow D_s^- K^+)_{\text{th}}}{d\mathcal{B}(\bar{B}^0 \rightarrow \pi^+ \ell^- \bar{\nu}_\ell)/dq^2|_{q^2=m_{D_s}^2}} = 6\pi^2 f_{D_s}^2 |V_{cs}|^2 |a_{1\text{eff}}^{KD_s}|^2 X_{SU(3)}, \quad (86)$$

where

$$X_{SU(3)} = \left(1 - \frac{m_K^2}{m_{B_s}^2}\right)^2 \frac{\left[\Phi\left(\frac{m_K}{m_{B_s}}, \frac{m_{D_s}}{m_{B_s}}\right)\right]}{\left[\Phi\left(\frac{m_\pi}{m_B}, \frac{m_{D_s}}{m_{B_s}}\right)\right]^3} \left[\frac{F_0^{B_s \rightarrow K}(m_{D_s}^2)}{F_1^{B \rightarrow \pi}(m_{D_s}^2)}\right]^2. \quad (87)$$

It should be noted that different phase-space factors enter in this expression, in contrast to the decay ratios considered above. The ratio of form factors can be expressed as

$$\left[\frac{F_0^{B_s \rightarrow K}(m_{D_s}^2)}{F_1^{B \rightarrow \pi}(m_{D_s}^2)}\right]^2 = \left[\frac{F_0^{B_s \rightarrow K}(m_{D_s}^2)}{F_1^{B_s \rightarrow K}(m_{D_s}^2)}\right]^2 \left[\frac{F_1^{B_s \rightarrow K}(m_{D_s}^2)}{F_1^{B \rightarrow \pi}(m_{D_s}^2)}\right]^2. \quad (88)$$

The non-perturbative form factors have been determined with lattice QCD [51, 52] and QCD light-cone sum rule analyses [34, 53]. In view of the currently large experimental uncertainty of  $\mathcal{B}(\bar{B}_s^0 \rightarrow D_s^- K^+)_{\text{th}}$ , we assume that the first ratio still satisfies the relation in Eq. (71) for  $q^2 = m_{D_s}^2$ , i.e. is close to 1, which is actually in agreement with the analysis in Ref. [54]. The second form-factor ratio represents the  $SU(3)$ -breaking corrections, and was calculated in Ref. [34] with the following result:

$$\left[\frac{F_1^{B_s \rightarrow K}(m_{D_s}^2)}{F_1^{B \rightarrow \pi}(m_{D_s}^2)}\right] = 1.12 \pm 0.02. \quad (89)$$

Using the theoretical branching ratio for the  $\bar{B}_s^0 \rightarrow D_s^- K^+$  decay in Table 2 and the following experimental value of the differential semileptonic branching ratio [10]:

$$d\mathcal{B}(\bar{B}^0 \rightarrow \pi^+ \ell^- \bar{\nu}_\ell)/dq^2|_{q^2=m_{D_s}^2} = (7.14 \pm 0.46) \times 10^{-6} \text{ GeV}^{-2}, \quad (90)$$

we obtain

$$R_{K^+D_s^-} = 3.64 \pm 1.70, \quad (91)$$

yielding

$$|a_{1\text{eff}}^{KD_s}| = 0.77 \pm 0.18 \quad (92)$$

with the help of the expressions given above. Assuming  $r_E^{KD_s} = r_E^{D_sK}$  with the numerical value for the latter parameter in Eq. (81) yields

$$|a_1^{KD_s}| = 0.77 \pm 0.19. \quad (93)$$

In comparison with Eq. (82), the uncertainty is now significantly larger. However, we find again a similar pattern, with a central value smaller than the theoretical reference value in Eq. (63). Although factorisation may not work as well as in the  $\bar{B}_s^0 \rightarrow D_s^+ K^-$  decay, this is yet another intriguing observation. It would be very important and interesting to reduce the corresponding uncertainties, both the theoretical and the experimental ones, and to have a measurement of the differential  $\bar{B}_s^0 \rightarrow K_s^+ \ell \bar{\nu}_\ell$  decay rate available.

### 3.5 Puzzling Patterns

Let us now complement the results for the  $|a_1|$  parameters of the  $\bar{B}_s^0 \rightarrow D_s^+ K^-$  and  $\bar{B}_s^0 \rightarrow D_s^- K^+$  channels obtained in Section 3.4 with the picture arising for decays with similar dynamics. As we have seen in Section 3.3, the decay  $\bar{B}_d^0 \rightarrow D_d^+ K^-$  originates from  $b \rightarrow c\bar{u}s$  processes in analogy to the  $\bar{B}_s^0 \rightarrow D_s^+ K^-$  channel but does not receive contributions from exchange topologies. Introducing

$$R_{D_d^+K^-} \equiv \frac{\mathcal{B}(\bar{B}_d^0 \rightarrow D_d^+ K^-)}{d\mathcal{B}(\bar{B}_d^0 \rightarrow D_d^+ \ell^- \bar{\nu}_\ell)/dq^2|_{q^2=m_K^2}} = 6\pi^2 f_K^2 |V_{us}|^2 |a_1^{D_dK}|^2 X_{D_dK} \quad (94)$$

with

$$X_{D_dK} = \frac{(m_{B_d}^2 - m_{D_d}^2)^2}{[m_{B_d}^2 - (m_{D_d} + m_K)^2][m_{B_d}^2 - (m_{D_d} - m_K)^2]} \left[ \frac{F_0^{B_d \rightarrow D_d}(m_K^2)}{F_1^{B_d \rightarrow D_d}(m_K^2)} \right]^2, \quad (95)$$

which are the counterparts of Eqs. (74) and (75), we may extract  $|a_1^{D_dK}|$  from the data. Applying the CLN parametrisation [48] with the following parameters [10]:

$$\eta_{\text{EW}} G(1) |V_{cb}| = (42.00 \pm 1.00) \times 10^{-3}, \quad \rho^2 = 1.131 \pm 0.033, \quad (96)$$

and using the lifetime  $\tau_{B_d}$  in Eq. (45), we get the following result for the differential branching ratio at the relevant value of  $q^2 = m_K^2$ :

$$d\mathcal{B}(\bar{B}_d^0 \rightarrow D_d^+ \ell^- \bar{\nu}_\ell)/dq^2|_{q^2=m_K^2} = (3.65 \pm 0.23) \times 10^{-3} \text{ GeV}^{-2}. \quad (97)$$

Using the form-factor ratio

$$\left[ \frac{F_0^{B_d \rightarrow D_d}(m_K^2)}{F_1^{B_d \rightarrow D_d}(m_K^2)} \right] = 1 \quad (98)$$

in accordance with the normalisation condition (71), we obtain

$$|a_1^{D_d K}| = 0.83 \pm 0.05, \quad (99)$$

which should be compared with the corresponding theoretical value in Eq. (55). We observe that the experimental central value is again significantly smaller, and encounter a discrepancy at the  $4.8\sigma$  level.

For the  $U$ -spin partner  $\bar{B}_d^0 \rightarrow D_d^+ \pi^-$  of the  $\bar{B}_s^0 \rightarrow D_s^+ K^-$  channel [2], we introduce

$$R_{D^+ \pi^-} \equiv \frac{\mathcal{B}(\bar{B}_d^0 \rightarrow D_d^+ \pi^-)}{d\mathcal{B}(\bar{B}_d^0 \rightarrow D_d^+ \ell^- \bar{\nu}_\ell) / dq^2|_{q^2=m_\pi^2}} = 6\pi^2 f_\pi^2 |V_{ud}|^2 |a_{1\text{eff}}^{D_d \pi}|^2 X_{D_d \pi} \quad (100)$$

with

$$X_{D_d \pi} = \frac{(m_{B_d}^2 - m_{D_d}^2)^2}{[m_{B_d}^2 - (m_{D_d} + m_\pi)^2][m_{B_d}^2 - (m_{D_d} - m_\pi)^2]} \left[ \frac{F_0^{B_d \rightarrow D_d}(m_\pi^2)}{F_1^{B_d \rightarrow D_d}(m_\pi^2)} \right]^2, \quad (101)$$

where

$$a_{1\text{eff}}^{D_d \pi} = a_1^{D_d \pi} \left( 1 + \frac{E_{D_d \pi}}{T_{D_d \pi}} \right) \quad (102)$$

takes also the exchange topology into account. Using  $f_\pi |V_{ud}| = (127.13 \pm 0.02)$  MeV [46] and the experimental differential semileptonic branching ratio for  $q^2 = m_\pi^2$  [10],

$$d\mathcal{B}(\bar{B}_d^0 \rightarrow D_d^+ \ell^- \bar{\nu}_\ell) / dq^2|_{q^2=m_\pi^2} = (3.80 \pm 0.24) \times 10^{-3} \text{ GeV}^{-2}, \quad (103)$$

we find

$$|a_{1\text{eff}}^{D_d \pi}| = 0.83 \pm 0.03. \quad (104)$$

If we assume  $r_E^{D_d \pi} = r_E^{D_s K}$  with the numerical value in Eq. (81), we get

$$|a_1^{D_d \pi}| = 0.83 \pm 0.07, \quad (105)$$

which should be compared with the theoretical prediction in Eq. (55). We observe again that the experimental value is much smaller, with a discrepancy at the  $3.3\sigma$  level.

The  $\bar{B}_s^0 \rightarrow D_s^+ \pi^-$  decay differs from  $\bar{B}_d^0 \rightarrow D_d^+ \pi^-$  only through the spectator quarks, and does not receive contributions from exchange topologies, thereby representing a cleaner setting. In analogy to the discussion above, we introduce the ratio

$$R_{D_s^+ \pi^-} \equiv \frac{\mathcal{B}(\bar{B}_s^0 \rightarrow D_s^+ \pi^-)_{\text{th}}}{d\mathcal{B}(\bar{B}_s^0 \rightarrow D_s^+ \ell^- \bar{\nu}_\ell) / dq^2|_{q^2=m_\pi^2}} = 6\pi^2 f_\pi^2 |V_{ud}|^2 |a_1^{D_s \pi}|^2 X_{D_s \pi} \quad (106)$$

with

$$X_{D_s \pi} = \frac{(m_{B_s}^2 - m_{D_s}^2)^2}{[m_{B_s}^2 - (m_{D_s} + m_\pi)^2][m_{B_s}^2 - (m_{D_s} - m_\pi)^2]} \left[ \frac{F_0^{B_s \rightarrow D_s}(m_\pi^2)}{F_1^{B_s \rightarrow D_s}(m_\pi^2)} \right]^2. \quad (107)$$

Using Eqs. (49) and (50), we find  $\mathcal{B}(\bar{B}_s^0 \rightarrow D_s^+ \pi^-)_{\text{th}} = (2.99 \pm 0.23) \times 10^{-3}$ . Concerning the differential rate of the semileptonic  $\bar{B}_s^0 \rightarrow D_s^+ \ell^- \bar{\nu}_\ell$  decay, we apply again the parameters of the CLN parametrisation given by the LHCb collaboration in Ref. [47] with the  $\bar{B}_s^0$  lifetime in Eq. (45), yielding

$$d\mathcal{B}(\bar{B}_s^0 \rightarrow D_s^+ \ell^- \bar{\nu}_\ell) / dq^2|_{q^2=m_\pi^2} = (4.12 \pm 0.46) \times 10^{-3} \text{ GeV}^{-2}. \quad (108)$$

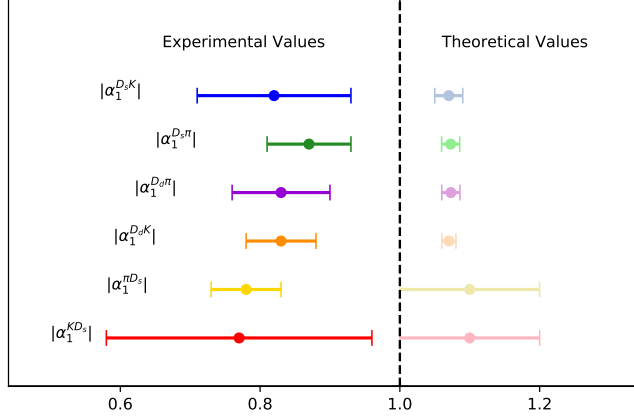


Figure 2: Experimental and theoretical SM values of the  $|a_1|$  parameters for various decay processes as discussed in the text.

Finally, we extract the following result from the data:

$$|a_1^{D_s \pi}| = 0.87 \pm 0.06. \quad (109)$$

Comparing this value with the theoretical prediction in Eq. (55), we observe that it is again too small, differing at the  $3.2\sigma$  level.

Finally, we consider the  $\bar{B}_d^0 \rightarrow \pi^+ D_s^-$  decay, which is the counterpart of  $\bar{B}_s^0 \rightarrow K^+ D_s^-$  and differs only through the spectator quarks. In particular, this mode does not have an exchange contribution. Introducing

$$R_{\pi^+ D_s^-} \equiv \frac{\mathcal{B}(\bar{B}_d^0 \rightarrow \pi^+ D_s^-)}{d\mathcal{B}(\bar{B}^0 \rightarrow \pi^+ \ell^- \bar{\nu}_\ell) / dq^2|_{q^2=m_{D_s}^2}} = 6\pi^2 f_{D_s}^2 |V_{cs}|^2 |a_1^{\pi D_s}|^2 X_{\pi D_s} \quad (110)$$

with

$$X_{\pi D_s} = \frac{(m_{B_d}^2 - m_\pi^2)^2}{[m_{B_d}^2 - (m_\pi + m_{D_s})^2][m_{B_d}^2 - (m_\pi - m_{D_s})^2]} \left[ \frac{F_0^{B_d \rightarrow \pi}(m_{D_s}^2)}{F_1^{B_d \rightarrow \pi}(m_{D_s}^2)} \right]^2, \quad (111)$$

we find

$$|a_1^{\pi D_s}| = 0.78 \pm 0.05, \quad (112)$$

where we have used the experimental differential branching ratio [10]:

$$d\mathcal{B}(\bar{B}^0 \rightarrow \pi^+ \ell^- \bar{\nu}_\ell) / dq^2|_{q^2=m_{D_s}^2} = (7.14 \pm 0.46) \times 10^{-6} \text{ GeV}^{-2}. \quad (113)$$

In comparison with Eq. (93), we have a consistent result although with significantly smaller uncertainty. The theoretical reference value in Eq. (65) differs from the experimental result at the  $2.9\sigma$  level.

In Fig. 2, we show our results for the various  $|a_1|$  parameters determined from the experimental data and compare them with the theoretical SM expectations. A similar pattern with values of  $|a_1|$  smaller than one was found for  $\bar{B}_d^0 \rightarrow D_d^+ \pi^-$  and  $\bar{B}_d^0 \rightarrow D_d^+ K^-$  decays in Ref. [14], and has recently been identified and discussed in more detail within

QCD factorisation also for  $\bar{B}_s^0 \rightarrow D_s^+ \pi^-$  in Ref. [15]. This feature has led to recent analyses within scenarios for physics beyond the SM [17–19].

The picture of the  $|a_1|$  parameters of the  $b \rightarrow c$  transitions is very intriguing, showing puzzling patterns with respect to the SM predictions of QCD factorisation. These decays are prime examples where this framework is expected to work very well. Even in the  $\bar{B}_s^0 \rightarrow K^+ D_s^-$  and  $\bar{B}_d^0 \rightarrow \pi^+ D_s^-$  channels, where factorisation is on less solid ground, we find indications of a similar pattern (see also Ref. [3]). Interestingly, in our analysis in Section 3.3, we did not find any indication for an anomalous enhancement of the exchange topologies, which could – in principle – arise from large non-factorisable effects. A picture in favour of factorisation is also supported by the small strong phase  $\delta_s$  in Eq. (23).

These observations are particularly exciting in view of the puzzling result for  $\gamma$  which follows from the analysis of the CP-violating observables of the  $\bar{B}_s^0 \rightarrow D_s^\mp K^\pm$  decays in Section 2. Could they have a similar origin, arising from physics beyond the SM? Let us now generalise our discussion of the  $\bar{B}_s^0 \rightarrow D_s^\mp K^\pm$  system to include NP effects.

## 4 In Pursuit of New Physics

### 4.1 New Physics Amplitudes

The starting point of our analysis of NP effects is to generalise the transition amplitudes. Let us first have a look at the  $\bar{B}_s^0$  and  $B_s^0$  decays into the final state  $D_s^+ K^-$ . We may write the corresponding decay amplitudes as follows:

$$A(\bar{B}_s^0 \rightarrow D_s^+ K^-) = A(\bar{B}_s^0 \rightarrow D_s^+ K^-)_{\text{SM}} \left[ 1 + \bar{\rho} e^{i\bar{\delta}} e^{i\bar{\varphi}} \right] \quad (114)$$

$$A(B_s^0 \rightarrow D_s^+ K^-) = A(B_s^0 \rightarrow D_s^+ K^-)_{\text{SM}} \left[ 1 + \rho e^{i\delta} e^{-i\varphi} \right]. \quad (115)$$

Here  $\bar{\rho}$  and  $\rho$  describe the strength of the NP contributions to  $b \rightarrow c\bar{u}s$  and  $\bar{b} \rightarrow \bar{u}c\bar{s}$  quark-level transitions with respect to the corresponding SM amplitudes, respectively, with  $\bar{\delta}$ ,  $\delta$  denoting CP-conserving strong phases while  $\bar{\varphi}$ ,  $\varphi$  are CP-violating NP phases:

$$\bar{\rho} e^{i\bar{\delta}} e^{i\bar{\varphi}} \equiv \frac{A(\bar{B}_s^0 \rightarrow D_s^+ K^-)_{\text{NP}}}{A(\bar{B}_s^0 \rightarrow D_s^+ K^-)_{\text{SM}}}, \quad \rho e^{i\delta} e^{-i\varphi} \equiv \frac{A(B_s^0 \rightarrow D_s^+ K^-)_{\text{NP}}}{A(B_s^0 \rightarrow D_s^+ K^-)_{\text{SM}}}. \quad (116)$$

These parameterisations of NP effects are actually more general than they may look at first sight, applying to situations where various NP contributions to the given quark-level transitions have the same CP-conserving or CP-violating phases.

The amplitudes for the CP-conjugate decay processes take the form

$$A(B_s^0 \rightarrow D_s^- K^+) = A(B_s^0 \rightarrow D_s^- K^+)_{\text{SM}} \left[ 1 + \bar{\rho} e^{i\bar{\delta}} e^{-i\bar{\varphi}} \right] \quad (117)$$

$$A(\bar{B}_s^0 \rightarrow D_s^- K^+) = A(\bar{B}_s^0 \rightarrow D_s^- K^+)_{\text{SM}} \left[ 1 + \rho e^{i\delta} e^{i\varphi} \right] \quad (118)$$

with

$$|A(\bar{B}_s^0 \rightarrow D_s^+ K^-)_{\text{SM}}| = |A(B_s^0 \rightarrow D_s^- K^+)_{\text{SM}}| \quad (119)$$

$$|A(B_s^0 \rightarrow D_s^+ K^-)_{\text{SM}}| = |A(\bar{B}_s^0 \rightarrow D_s^- K^+)_{\text{SM}}|, \quad (120)$$

reflecting the absence of direct CP violation in these decays in the SM. Introducing the CP asymmetries

$$\bar{\mathcal{A}}_{\text{CP}}^{\text{dir}} \equiv \frac{|A(B_s^0 \rightarrow D_s^- K^+)|^2 - |A(\bar{B}_s^0 \rightarrow D_s^+ K^-)|^2}{|A(B_s^0 \rightarrow D_s^- K^+)|^2 + |A(\bar{B}_s^0 \rightarrow D_s^+ K^-)|^2} \quad (121)$$

$$\mathcal{A}_{\text{CP}}^{\text{dir}} \equiv \frac{|A(B_s^0 \rightarrow D_s^+ K^-)|^2 - |A(\bar{B}_s^0 \rightarrow D_s^- K^+)|^2}{|A(B_s^0 \rightarrow D_s^+ K^-)|^2 + |A(\bar{B}_s^0 \rightarrow D_s^- K^+)|^2}, \quad (122)$$

we obtain

$$\bar{\mathcal{A}}_{\text{CP}}^{\text{dir}} = \frac{2\bar{\rho} \sin \bar{\delta} \sin \bar{\varphi}}{1 + 2\bar{\rho} \cos \bar{\delta} \cos \bar{\varphi} + \bar{\rho}^2}, \quad \mathcal{A}_{\text{CP}}^{\text{dir}} = \frac{2\rho \sin \delta \sin \varphi}{1 + 2\rho \cos \delta \cos \varphi + \rho^2}. \quad (123)$$

Consequently, we observe that NP may generate non-vanishing direct CP asymmetries, provided we have non-vanishing CP-conserving and CP-violating phases.

Concerning the ratios  $R_{D_s^+ K^-}$  and  $R_{K^+ D_s^-}$  introduced in Eqs. (72) and (83), respectively, it is useful to generalize them through the following CP-averaged quantities:

$$\langle R_{D_s K} \rangle \equiv \frac{\mathcal{B}(\bar{B}_s^0 \rightarrow D_s^+ K^-)_{\text{th}} + \mathcal{B}(B_s^0 \rightarrow D_s^- K^+)_{\text{th}}}{[\text{d}\mathcal{B}(\bar{B}_s^0 \rightarrow D_s^+ \ell^- \bar{\nu}_\ell) / \text{d}q^2 + \text{d}\mathcal{B}(B_s^0 \rightarrow D_s^- \ell^+ \nu_\ell) / \text{d}q^2] |_{q^2=m_K^2}} \quad (124)$$

$$\langle R_{K D_s} \rangle \equiv \frac{\mathcal{B}(\bar{B}_s^0 \rightarrow K^+ D_s^-)_{\text{th}} + \mathcal{B}(B_s^0 \rightarrow K^- D_s^+)_{\text{th}}}{[\text{d}\mathcal{B}(\bar{B}_s^0 \rightarrow K^+ \ell^- \bar{\nu}_\ell) / \text{d}q^2 + \text{d}\mathcal{B}(B_s^0 \rightarrow K^- \ell^+ \nu_\ell) / \text{d}q^2] |_{q^2=m_{D_s}^2}}. \quad (125)$$

In the case of vanishing direct CP violation in the corresponding modes, as in the SM considered in Subsection 3.4, we have  $\langle R_{D_s K} \rangle = R_{D_s^+ K^-}$  and  $\langle R_{K D_s} \rangle = R_{K^+ D_s^-}$ . In the presence of NP contributions, it is useful to introduce the following quantities:

$$\bar{b} \equiv \frac{\langle R_{D_s K} \rangle}{6\pi^2 f_K^2 |V_{us}|^2 |a_{1\text{eff}}^{D_s K}|^2 X_{D_s K}} = \frac{\langle \mathcal{B}(\bar{B}_s^0 \rightarrow D_s^+ K^-)_{\text{th}} \rangle}{\mathcal{B}(\bar{B}_s^0 \rightarrow D_s^+ K^-)_{\text{th}}^{\text{SM}}} = 1 + 2\bar{\rho} \cos \bar{\delta} \cos \bar{\varphi} + \bar{\rho}^2 \quad (126)$$

$$b \equiv \frac{\langle R_{K D_s} \rangle}{6\pi^2 f_{D_s}^2 |V_{cs}|^2 |a_{1\text{eff}}^{K D_s}|^2 X_{K D_s}} = \frac{\langle \mathcal{B}(\bar{B}_s^0 \rightarrow K^+ D_s^-)_{\text{th}} \rangle}{\mathcal{B}(\bar{B}_s^0 \rightarrow K^+ D_s^-)_{\text{th}}^{\text{SM}}} = 1 + 2\rho \cos \delta \cos \varphi + \rho^2, \quad (127)$$

which allow us to probe the NP parameters, utilising the theoretical expectations of the parameters  $|a_1^{D_s K}|$  and  $|a_1^{K D_s}|$  with  $r_E^{D_s K}$  and  $r_E^{K D_s}$ , respectively, as input.

Employing the direct CP asymmetry  $\mathcal{A}_{\text{CP}}^{\text{dir}}$  and the branching ratio observable  $b$ , we may determine  $\rho$  as function of the CP-violating phase  $\varphi$  with the help of

$$\rho = \sqrt{u \pm \sqrt{u^2 - w}}, \quad (128)$$

where

$$u \equiv b - 1 + 2 \cos^2 \varphi \quad (129)$$

and

$$w \equiv (b - 1)^2 + \left( \frac{b \mathcal{A}_{\text{CP}}^{\text{dir}}}{\tan \varphi} \right)^2. \quad (130)$$

Similar expressions hold for the CP-conjugate quantities, allowing the extraction of the NP parameter  $\bar{\rho}$  as function of  $\bar{\varphi}$ .

## 4.2 Interference Effects Through $B_s^0-\bar{B}_s^0$ Mixing

For the CP-violating phenomena in the  $B_s^0 \rightarrow D_s^\mp K^\pm$  system, interference effects between the different decay paths through  $B_s^0-\bar{B}_s^0$  mixing play the essential role, as we have seen in Section 2. Let us now generalise these considerations to allow for NP contributions with new sources of CP violation. The key information is encoded in the observables  $\xi$  and  $\bar{\xi}$ , which we may write using Eqs. (7) and (8) with (117) and (118) as follows:

$$\xi = -e^{-i(\phi_s+\gamma)} \left[ \frac{1}{x_s e^{i\delta_s}} \right] \left[ \frac{1 + \bar{\rho} e^{i\bar{\delta}} e^{+i\bar{\varphi}}}{1 + \rho e^{i\delta} e^{-i\varphi}} \right] = -|\xi| e^{-i\delta_s} e^{-i(\phi_s+\gamma)} e^{i\Delta\varphi} \quad (131)$$

$$\bar{\xi} = -e^{-i(\phi_s+\gamma)} [x_s e^{i\delta_s}] \left[ \frac{1 + \rho e^{i\delta} e^{+i\varphi}}{1 + \bar{\rho} e^{i\bar{\delta}} e^{-i\bar{\varphi}}} \right] = -|\bar{\xi}| e^{+i\delta_s} e^{-i(\phi_s+\gamma)} e^{i\Delta\bar{\varphi}}, \quad (132)$$

where

$$\tan \Delta\varphi = \frac{\rho \sin(\varphi - \delta) + \bar{\rho} \sin(\bar{\varphi} + \bar{\delta}) + \bar{\rho} \rho \sin(\bar{\delta} - \delta + \bar{\varphi} + \varphi)}{1 + \rho \cos(\varphi - \delta) + \bar{\rho} \cos(\bar{\varphi} + \bar{\delta}) + \bar{\rho} \rho \cos(\bar{\delta} - \delta + \bar{\varphi} + \varphi)} \quad (133)$$

and

$$\tan \Delta\bar{\varphi} = \frac{\bar{\rho} \sin(\bar{\varphi} - \bar{\delta}) + \rho \sin(\varphi + \delta) + \rho \bar{\rho} \sin(\delta - \bar{\delta} + \varphi + \bar{\varphi})}{1 + \bar{\rho} \cos(\bar{\varphi} - \bar{\delta}) + \rho \cos(\varphi + \delta) + \rho \bar{\rho} \cos(\delta - \bar{\delta} + \varphi + \bar{\varphi})}. \quad (134)$$

Since the hadronic parameter  $x_s$  with its CP-conserving strong phase  $\delta_s$  cancels in the product of these observables, this combination is central for studying CP violation:

$$\xi \times \bar{\xi} = e^{-i2(\phi_s+\gamma)} \left[ \frac{1 + \rho e^{i\delta} e^{+i\varphi}}{1 + \rho e^{i\delta} e^{-i\varphi}} \right] \left[ \frac{1 + \bar{\rho} e^{i\bar{\delta}} e^{+i\bar{\varphi}}}{1 + \bar{\rho} e^{i\bar{\delta}} e^{-i\bar{\varphi}}} \right]. \quad (135)$$

Using the relation

$$\frac{1 + \rho e^{i\delta} e^{+i\varphi}}{1 + \rho e^{i\delta} e^{-i\varphi}} = e^{-i\Delta\Phi} \sqrt{\frac{1 - \mathcal{A}_{\text{CP}}^{\text{dir}}}{1 + \mathcal{A}_{\text{CP}}^{\text{dir}}}} \quad (136)$$

with

$$\cos \Delta\Phi = \sqrt{\frac{1 - \mathcal{A}_{\text{CP}}^{\text{dir}}}{1 + \mathcal{A}_{\text{CP}}^{\text{dir}}}} \left[ \frac{1 + 2\rho \cos \delta \cos \varphi + \rho^2 \cos 2\varphi}{1 + 2\rho \cos(\delta - \varphi) + \rho^2} \right] \quad (137)$$

and

$$\tan \Delta\Phi = - \left[ \frac{2\rho \cos \delta \sin \varphi + \rho^2 \sin 2\varphi}{1 + 2\rho \cos \delta \cos \varphi + \rho^2 \cos 2\varphi} \right], \quad (138)$$

as well as the corresponding counterparts for the phase  $\Delta\bar{\Phi}$  that are related to  $\bar{\rho}$ ,  $\bar{\varphi}$  and  $\bar{\mathcal{A}}_{\text{CP}}^{\text{dir}}$  in an analogous way, we obtain

$$\xi \times \bar{\xi} = e^{-i2(\phi_s+\gamma)} \sqrt{\left[ \frac{1 - \mathcal{A}_{\text{CP}}^{\text{dir}}}{1 + \mathcal{A}_{\text{CP}}^{\text{dir}}} \right] \left[ \frac{1 - \bar{\mathcal{A}}_{\text{CP}}^{\text{dir}}}{1 + \bar{\mathcal{A}}_{\text{CP}}^{\text{dir}}} \right]} e^{-i(\Delta\Phi + \Delta\bar{\Phi})}, \quad (139)$$

where the CP-violating NP phase shifts satisfy the sum rule

$$\Delta\Phi + \Delta\bar{\Phi} = -(\Delta\varphi + \Delta\bar{\varphi}). \quad (140)$$

Let us simplify the expression in Eq. (139) further using the observable  $C$  in Eq. (10) and its CP-conjugate. Writing

$$|\xi \times \bar{\xi}|^2 = \left[ \frac{1 - \mathcal{A}_{\text{CP}}^{\text{dir}}}{1 + \mathcal{A}_{\text{CP}}^{\text{dir}}} \right] \left[ \frac{1 - \bar{\mathcal{A}}_{\text{CP}}^{\text{dir}}}{1 + \bar{\mathcal{A}}_{\text{CP}}^{\text{dir}}} \right] = 1 + \epsilon, \quad (141)$$

we obtain

$$-\frac{1}{2}\epsilon = \frac{C + \bar{C}}{(1 + C)(1 + \bar{C})} = \mathcal{A}_{\text{CP}}^{\text{dir}} + \bar{\mathcal{A}}_{\text{CP}}^{\text{dir}} + \mathcal{O}((\mathcal{A}_{\text{CP}}^{\text{dir}})^2), \quad (142)$$

generalising the relation in Eq. (12) which was assumed by the LHCb collaboration in Ref. [9]. Finally, we arrive at the following expression:

$$\xi \times \bar{\xi} = \sqrt{1 - 2 \left[ \frac{C + \bar{C}}{(1 + C)(1 + \bar{C})} \right]} e^{-i[2(\phi_s + \gamma) + \Delta\Phi + \Delta\bar{\Phi}]}. \quad (143)$$

This is the generalisation of Eq. (9). The corresponding product of  $\xi$  and  $\bar{\xi}$  can still be determined through the observables of the time-dependent rate asymmetries of the  $B_s^0 \rightarrow D_s^\mp K^\pm$  system. We observe that possible corrections to the relations in Eqs. (11) and (12) are now manifestly included, and that the UT angle  $\gamma$  actually enters with a shift due to the CP-violating NP phases, thereby resulting in the “effective” angle

$$\gamma_{\text{eff}} \equiv \gamma + \frac{1}{2}(\Delta\Phi + \Delta\bar{\Phi}) = \gamma - \frac{1}{2}(\Delta\varphi + \Delta\bar{\varphi}). \quad (144)$$

In the future, it would be important to generalise the experimental analyses of the  $\bar{B}_s^0 \rightarrow D_s^+ K^-$  and  $B_s^0 \rightarrow D_s^+ K^-$  decays and their CP conjugates correspondingly.

## 4.3 New Physics Analysis of the Data

### 4.3.1 Preliminaries

Let us now apply the model-independent formalism developed above and come back to the intriguing patterns in the data that we encountered in Sections 2 and 3, interpreting them in terms of NP contributions with new sources of CP violation. In order to have a scenario in agreement with the relation in Eq. (12), which was assumed by LHCb in Ref. [9], we make the following assumption:

$$\delta = \bar{\delta} = 0^\circ. \quad (145)$$

It implies vanishing direct CP asymmetries  $\bar{\mathcal{A}}_{\text{CP}}^{\text{dir}}$  and  $\mathcal{A}_{\text{CP}}^{\text{dir}}$ , as can be seen in Eq. (123), which would be consistent with the measurements of such observables in tree-diagram-like decays of the kind  $B \rightarrow DK$  within the current uncertainties [11].

In such a scenario, the NP amplitude would enter with the same CP-conserving strong phase as the SM amplitude, which may actually well be the case. We will describe possible relative minus signs through the CP-violating phases  $\varphi$  and  $\bar{\varphi}$ , i.e. through terms of  $180^\circ$ . The strong phases would be generated through non-factorisable effects arising in the hadronic matrix elements of four-quark operators. In view of the discussion of factorisation in Subsection 3.3, we would expect smallish phases for the decays at hand, in particular for the  $b \rightarrow c$  mode  $\bar{B}_s^0 \rightarrow D_s^+ K^-$ . The result for the strong phase difference  $\delta_s$  in Eq. (23) would be fully consistent with this picture within the uncertainties.



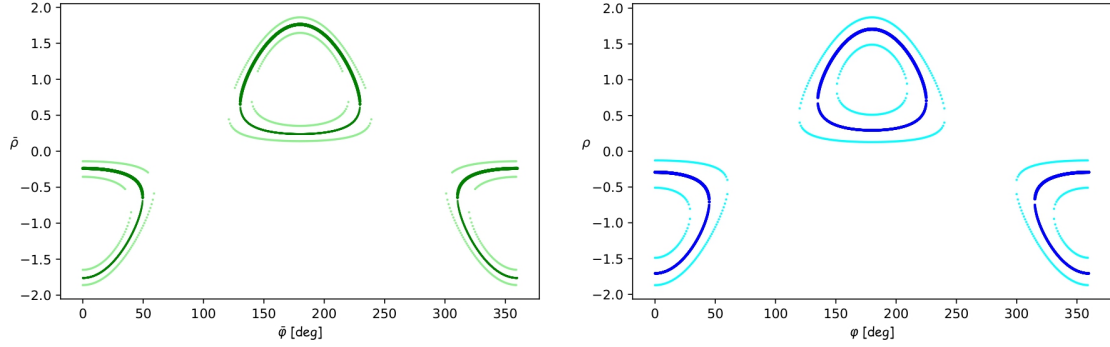


Figure 3: In the left panel, we show  $\bar{\rho}$  as function of the CP-violating phase  $\bar{\varphi}$ , following from the branching ratio observable  $\bar{b}$ . In the right panel, we show the corresponding analysis for  $\rho$  and  $\varphi$ , using  $b$ .

### 4.3.2 New Physics Parameter Correlations

As the first observables, we consider the branching ratio information encoded in Eqs. (126) and (127). Assuming the relation in Eq. (145), we obtain the expressions

$$\bar{\rho} = -\cos \bar{\varphi} \pm \sqrt{\bar{b} - \sin^2 \bar{\varphi}} \quad (146)$$

$$\rho = -\cos \varphi \pm \sqrt{b - \sin^2 \varphi}, \quad (147)$$

which are in agreement with Eq. (128) for vanishing direct CP asymmetries. Using the experimental values in Eqs. (79) and (91) with the theoretical expectations of the  $|a_1|$  parameters in Eqs. (56) and (63), respectively, complemented with  $r_E^{KD_s} = r_E^{D_sK}$  for the numerical value of  $r_E^{D_sK}$  in (81), we obtain

$$|a_{1\text{eff}}^{D_sK}| = 1.07 \pm 0.09, \quad |a_{1\text{eff}}^{KD_s}| = 1.1 \pm 0.13, \quad (148)$$

yielding

$$\bar{b} = 0.58 \pm 0.16, \quad b = 0.50 \pm 0.26. \quad (149)$$

Finally, applying Eqs. (146) and (147), we get the constraints on the NP parameters shown in Fig. 3. Here the green (blue) contour shows the parameter  $\rho$  ( $\bar{\rho}$ ) as a function of the phase  $\varphi$  ( $\bar{\varphi}$ ) for the central value of the observable  $b$  ( $\bar{b}$ ). We include also the uncertainties, varying the values of the observable  $b$  ( $\bar{b}$ ) within the  $1\sigma$  range, which leads to the contours in lighter colours.

Let us now use in addition the observables of the time-dependent  $B_s^0 \rightarrow D_s^\mp K^\pm$  decay rates. Looking at Eqs. (133) and (134) with (144), we observe that Eq. (145) implies

$$\Delta\varphi = \Delta\bar{\varphi} = \gamma - \gamma_{\text{eff}} \quad (150)$$

with

$$\tan \Delta\varphi = \frac{\rho \sin \varphi + \bar{\rho} \sin \bar{\varphi} + \bar{\rho} \rho \sin(\bar{\varphi} + \varphi)}{1 + \rho \cos \varphi + \bar{\rho} \cos \bar{\varphi} + \bar{\rho} \rho \cos(\bar{\varphi} + \varphi)}. \quad (151)$$

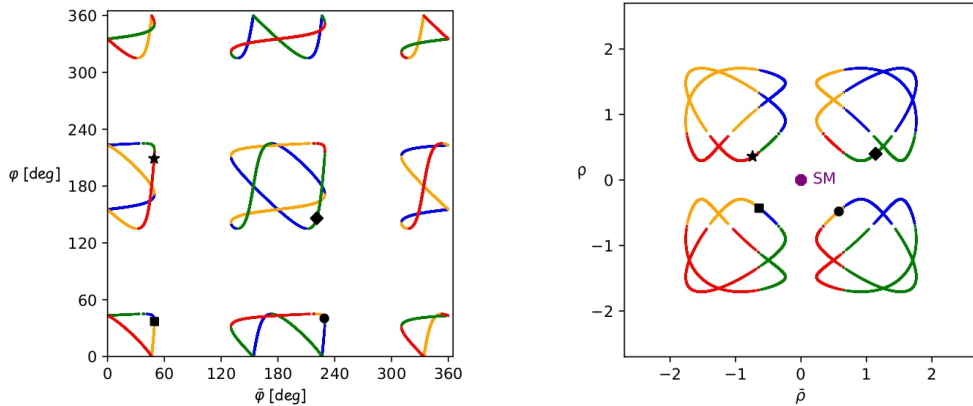


Figure 4: Correlations in the  $\bar{\varphi}$ - $\varphi$  plane (left) and the  $\bar{\rho}$ - $\rho$  plane (right) for the central values of the current data, as discussed in the text. We have indicated four illustrative points to show their appearance in the two correlations, and have made the SM point explicit.

Using the result in Eq. (24), which actually corresponds to the effective angle  $\gamma_{\text{eff}}$ , and applying  $\gamma = (70 \pm 7)^\circ$ , summarising the picture from analyses of CP violation in tree-level decays of the kind  $B \rightarrow DK$  [10], we obtain

$$\Delta\varphi = -(61 \pm 20)^\circ. \quad (152)$$

It should be emphasised that this NP phase shift was extracted in a *theoretically clean* way from the data. In particular, it does not rely on SM predictions of the observables  $\xi$  and  $\bar{\xi}$ , which is a very important feature and non-trivial finding.

Employing again  $\bar{b}$  and  $b$  (see Eqs. (146) and (147)), we may express  $\bar{\rho}$  and  $\rho$  in Eq. (151) as functions of  $\bar{\varphi}$  and  $\varphi$ , respectively, thereby allowing us to determine  $\varphi$  as a function of  $\bar{\varphi}$  from the experimental value of  $\Delta\varphi$  given in Eq. (152). With the help of Eqs. (146) and (147), we may then also determine the corresponding correlation in the  $\bar{\rho}$ - $\rho$  plane, where each point corresponds to a value of the CP-violating NP phase  $\bar{\varphi}$ .

In Fig. 4, we show the corresponding correlations for the central values of the current data. The contours in four different colours correspond to the four different combinations of the product  $\rho\bar{\rho}$  in Eq. (151), arising from the two possible values that each one of  $\rho$  and  $\bar{\rho}$  can take due to the different sign before the square root in Eqs. (146) and (147).

As examples, we pick some values from the correlation in the  $\bar{\varphi}$ - $\varphi$  plane and show the corresponding values in the  $\bar{\rho}$ - $\rho$  plane. We illustrate these points in Fig. 4 as a square, circle, diamond and star, corresponding to the following NP parameter sets:

$$(\rho, \varphi) = (-0.43, 37.0^\circ), \quad (\bar{\rho}, \bar{\varphi}) = (-0.64, 49.6^\circ) \quad (153)$$

$$(\rho, \varphi) = (-0.48, 40.3^\circ), \quad (\bar{\rho}, \bar{\varphi}) = (0.58, 229.0^\circ) \quad (154)$$

$$(\rho, \varphi) = (0.40, 146.0^\circ), \quad (\bar{\rho}, \bar{\varphi}) = (1.14, 221.0^\circ) \quad (155)$$

$$(\rho, \varphi) = (0.36, 209.0^\circ), \quad (\bar{\rho}, \bar{\varphi}) = (-0.74, 49.2^\circ). \quad (156)$$

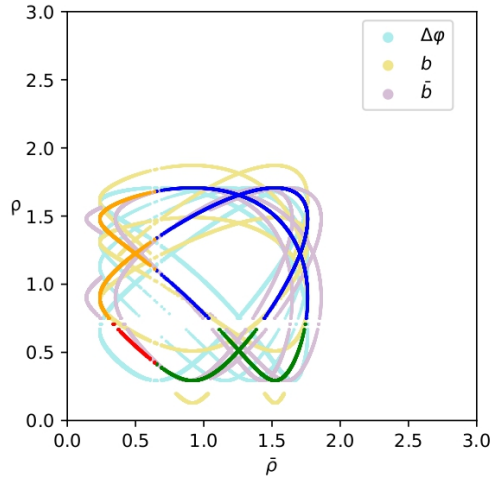


Figure 5: The correlations in the  $\bar{\rho}$ - $\rho$  plane including the uncertainties of the input quantities  $\bar{b}$ ,  $b$  and  $\Delta\varphi$ .

### 4.3.3 Discussion

In the correlations in the  $\bar{\varphi}$ - $\varphi$  plane, interestingly at least one of the CP-violating phases has to take a non-trivial value, thereby illustrating the need for new sources of CP violation. In the  $\bar{\rho}$ - $\rho$  plane, the SM point corresponding to the origin  $(0, 0)$  is excluded. The gaps between the various contours are in particular related to the values of  $\bar{b}$  and  $b$ , which are smaller than one, and arise from the algebraic structure of the underlying expressions. We notice that  $\rho$ ,  $\bar{\rho}$  are bounded to values below two. Interestingly, values as small as in the regime around 0.5 could accommodate the central values of the current data, thereby resolving the puzzling patterns in the measurements of CP violation as well as in the branching ratios. Here we would then have NP contributions at the level of 50% of the SM amplitudes. This feature is also nicely reflected by the NP parameter sets in Eqs. (153)–(156).

In Fig. 5, we illustrate the impact of the uncertainties of the input quantities  $\bar{b}$ ,  $b$  and  $\Delta\varphi$  on the contours in the  $\bar{\rho}$ - $\rho$  plane. Focusing only on the positive values of  $\rho$  and  $\bar{\rho}$ , we vary the values of each of the above three parameters separately and obtain the contours which are denoted with pale colours. Every different pale colour corresponds to one of the three parameters. We could now accommodate the data with NP contributions as small as about 30% of the SM amplitudes, which is an exciting observation.

In Refs. [17–19], specific NP scenarios which may affect  $B_{(s)} \rightarrow D_{(s)}\pi$  and  $B \rightarrow DK$  decays were recently discussed in view of the puzzling patterns in the branching ratios of these modes (see Section 3). Such kind of physics beyond the SM would also enter the  $B_s^0 \rightarrow D_s^\mp K^\pm$  system, which offers an exciting probe for CP-violating NP phases as we have demonstrated in our analysis.

## 5 Conclusions

Decays of  $\bar{B}_s^0$  and  $B_s^0$  mesons into the final state  $D_s^+ K^-$  and its CP conjugate  $D_s^- K^+$  provide an important laboratory for the testing the quark-flavour sector of the SM. Due to interference effects between these decay channels that are induced by  $B_s^0$ - $\bar{B}_s^0$  mixing, CP-violating asymmetries arise, which allow a clean determination of the UT angle  $\gamma$  within the SM. We have performed an analysis of LHCb measurements of these CP asymmetries, paying special attention to the resolution of discrete ambiguities. We have resolved a final discrete ambiguity, leaving us with  $\gamma = (131_{-22}^{+17})^\circ$ , where we have used a recent result for  $\phi_s$  taking penguin corrections into account. The large value of  $\gamma$  is surprising in view of the range around  $70^\circ$  following from tree decays of the kind  $B \rightarrow DK$  and global analyses of the UT.

Complementing the CP-violating observables with the measurement of an averaged branching ratio, we have extracted the individual branching ratios of the  $\bar{B}_s^0 \rightarrow D_s^+ K^-$  and  $B_s^0 \rightarrow D_s^- K^+$  decays from the data, thereby disentangling the interference effects between the different decay paths. In this analysis, we have also properly taken the effects of  $B_s^0$ - $\bar{B}_s^0$  mixing into account.

In the experimental study of the  $B_s^0 \rightarrow D_s^\mp K^\pm$  system, the LHCb collaboration has assumed that direct CP violation vanishes in these channels, as would be the case in the SM. However, NP effects with new sources of CP violation could actually generate such CP asymmetries. It would be interesting to constrain them experimentally in the future. We have presented the corresponding generalised formalism in this paper.

In order to minimise the impact of the uncertainties of hadronic form factors and the CKM matrix elements  $|V_{cb}|$  and  $|V_{ub}|$ , we have introduced ratios of the  $\bar{B}_s^0 \rightarrow D_s^+ K^-$  and  $\bar{B}_s^0 \rightarrow K^+ D_s^-$  branching ratios with the differential rates of semileptonic  $\bar{B}_s^0 \rightarrow D_s^+ \ell^- \bar{\nu}_\ell$  and  $\bar{B}_s^0 \rightarrow K^+ \ell^- \bar{\nu}_\ell$  decays, respectively. These quantities allow clean determinations of the parameters  $|a_1^{D_s K}|$  and  $|a_1^{K D_s}|$ , which characterise non-factorizable QCD effects. For the former  $b \rightarrow c$  mode, we find  $|a_1^{D_s K}| = 0.82 \pm 0.11$ . This value is intriguing as it differs at the  $2.2\sigma$  level from the theoretical expectation. In the case of  $\bar{B}_s^0 \rightarrow D_s^+ K^-$ , factorisation is expected to work very well, similar to  $\bar{B}_d^0 \rightarrow D_d^+ \pi^-$ ,  $\bar{B}_s^0 \rightarrow D_s^+ \pi^-$  and  $\bar{B}_d^0 \rightarrow D_d^+ K^-$  channels. Interestingly, in the latter decays, a similar pattern arises, as was found in the previous literature. We confirm this picture in the  $\bar{B}_s^0 \rightarrow D_s^+ K^-$  channel, thereby complementing the puzzling result for  $\gamma$  following from the CP asymmetries. In the case of the  $b \rightarrow u$  transition  $\bar{B}_s^0 \rightarrow K^+ D_s^-$ , the differential rate of the semileptonic partner  $\bar{B}_s^0 \rightarrow K^+ \ell^- \bar{\nu}_\ell$  has not yet been measured. However, replacing it through the  $SU(3)$ -related channel  $\bar{B}_d^0 \rightarrow \pi^+ \ell^- \bar{\nu}_\ell$ , we obtain  $|a_1^{K D_s}| = 0.77 \pm 0.19$ , showing a similar pattern as  $|a_1^{D_s K}|$ , although with larger uncertainty.

In view of the intriguing results for  $\gamma$  and the picture following from the branching ratios, we have generalised the analysis of the  $B_s^0 \rightarrow D_s^\mp K^\pm$  system to allow for NP contributions with new sources of CP violation. We have developed a model-independent formalism for the CP-violating observables to include also possible effects from direct CP violation, resulting finally in an effective angle  $\gamma_{\text{eff}}$  which differs from  $\gamma$  through a CP-violating NP phase shift. We have also generalised the expressions of the branching ratios of the underlying decay channels correspondingly.

In our NP analysis of the experimental data, we assume that CP-conserving phase differences vanish, which results in a setting consistent with the assumption made by the LHCb collaboration when measuring the observables. Applying our formalism, we have calculated correlations between the NP parameters of the  $b \rightarrow c\bar{u}s$  and  $b \rightarrow u\bar{c}s$  quark-level transitions. Interestingly, we obtain strongly correlated NP contributions with potentially large CP-violating phases. Moreover, we find that NP contributions as small as about 30% of the SM amplitudes could accommodate the current data.

The strategy presented in this paper sets the stage for analyses of future measurements of the  $B_s^0 \rightarrow D_s^\mp K^\pm$  system, employing also semileptonic  $\bar{B}_s^0 \rightarrow D_s^+ \ell^- \bar{\nu}_\ell$  and  $\bar{B}_s^0 \rightarrow K_s^+ \ell^- \bar{\nu}_\ell$  decays. It will be exciting to see how the data will evolve once we are moving to higher and higher precision. The burning question is whether we will finally be able to establish new sources of CP violation in the  $B_s^0 \rightarrow D_s^\mp K^\pm$  decays, which have been key players in this field since the pioneering days of  $B$  physics.

## Acknowledgements

We would like to thank Ruben Jaarsma and Philine van Vliet for useful discussions. This research has been supported by the Netherlands Organisation for Scientific Research (NWO).

## References

- [1] R. Aleksan, I. Dunietz and B. Kayser, *Z. Phys. C* **54** (1992), 653-660 doi:10.1007/BF01559494
- [2] R. Fleischer, *Nucl. Phys. B* **671** (2003), 459-482 doi:10.1016/j.nuclphysb.2003.08.010 [arXiv:hep-ph/0304027 [hep-ph]].
- [3] K. De Bruyn, R. Fleischer, R. Knegjens, M. Merk, M. Schiller and N. Tuning, *Nucl. Phys. B* **868** (2013), 351-367 doi:10.1016/j.nuclphysb.2012.11.012 [arXiv:1208.6463 [hep-ph]].
- [4] A. S. Dighe, I. Dunietz and R. Fleischer, *Eur. Phys. J. C* **6** (1999), 647-662 doi:10.1007/s100520050372 [arXiv:hep-ph/9804253 [hep-ph]].
- [5] I. Dunietz, R. Fleischer and U. Nierste, *Phys. Rev. D* **63** (2001), 114015 doi:10.1103/PhysRevD.63.114015 [arXiv:hep-ph/0012219 [hep-ph]].
- [6] S. Faller, R. Fleischer and T. Mannel, *Phys. Rev. D* **79** (2009), 014005 doi:10.1103/PhysRevD.79.014005 [arXiv:0810.4248 [hep-ph]].
- [7] K. De Bruyn and R. Fleischer, *JHEP* **03** (2015), 145 doi:10.1007/JHEP03(2015)145 [arXiv:1412.6834 [hep-ph]].

- [8] M. Z. Barel, K. De Bruyn, R. Fleischer and E. Malami, *J. Phys. G* **48** (2021) no.6, 065002 doi:10.1088/1361-6471/abf2a2 [arXiv:2010.14423 [hep-ph]].
- [9] R. Aaij *et al.* [LHCb], *JHEP* **03** (2018), 059 doi:10.1007/JHEP03(2018)059 [arXiv:1712.07428 [hep-ex]].
- [10] Y. S. Amhis *et al.* [HFLAV], *Eur. Phys. J. C* **81**, no.3, 226 (2021) doi:10.1140/epjc/s10052-020-8156-7 [arXiv:1909.12524 [hep-ex]].
- [11] P. A. Zyla *et al.* [Particle Data Group], *PTEP* **2020** (2020) no.8, 083C01 doi:10.1093/ptep/ptaa104
- [12] J. Charles, O. Deschamps, S. Descotes-Genon, H. Lacker, A. Menzel, S. Monteil, V. Niess, J. Ocariz, J. Orloff and A. Perez, *et al.* *Phys. Rev. D* **91** (2015) no.7, 073007 doi:10.1103/PhysRevD.91.073007 [arXiv:1501.05013 [hep-ph]].
- [13] UTfit collaboration, <http://www.utfit.org/UTfit/>.
- [14] R. Fleischer, N. Serra and N. Tuning, *Phys. Rev. D* **83** (2011), 014017 doi:10.1103/PhysRevD.83.014017 [arXiv:1012.2784 [hep-ph]].
- [15] M. Bordone, N. Gubernari, T. Huber, M. Jung and D. van Dyk, *Eur. Phys. J. C* **80**, no.10, 951 (2020) doi:10.1140/epjc/s10052-020-08512-8 [arXiv:2007.10338 [hep-ph]].
- [16] M. Beneke, G. Buchalla, M. Neubert and C. T. Sachrajda, *Nucl. Phys. B* **591**, 313-418 (2000) doi:10.1016/S0550-3213(00)00559-9 [arXiv:hep-ph/0006124 [hep-ph]].
- [17] S. Iguro and T. Kitahara, *Phys. Rev. D* **102** (2020) no.7, 071701 doi:10.1103/PhysRevD.102.071701 [arXiv:2008.01086 [hep-ph]].
- [18] F. M. Cai, W. J. Deng, X. Q. Li and Y. D. Yang, [arXiv:2103.04138 [hep-ph]].
- [19] M. Bordone, A. Greljo and D. Marzocca, *JHEP* **08** (2021), 036 doi:10.1007/JHEP08(2021)036 [arXiv:2103.10332 [hep-ph]].
- [20] J. Brod, A. Lenz, G. Tetlalmatzi-Xolocotzi and M. Wiebusch, *Phys. Rev. D* **92** (2015) no.3, 033002 doi:10.1103/PhysRevD.92.033002 [arXiv:1412.1446 [hep-ph]].
- [21] A. Lenz and G. Tetlalmatzi-Xolocotzi, *JHEP* **07** (2020), 177 doi:10.1007/JHEP07(2020)177 [arXiv:1912.07621 [hep-ph]].
- [22] K. De Bruyn, R. Fleischer, R. Knegjens, P. Koppenburg, M. Merk and N. Tuning, *Phys. Rev. D* **86** (2012), 014027 doi:10.1103/PhysRevD.86.014027 [arXiv:1204.1735 [hep-ph]].
- [23] J. D. Bjorken, *Nucl. Phys. Proc. Suppl.* **11**, 325 (1989).
- [24] M. J. Dugan and B. Grinstein, *Phys. Lett. B* **255**, 583 (1991).
- [25] M. Neubert and B. Stech, *Adv. Ser. Direct. High Energy Phys.* **15** (1998), 294-344 doi:10.1142/9789812812667\_0004 [arXiv:hep-ph/9705292 [hep-ph]].

- [26] C. W. Bauer, D. Pirjol and I. W. Stewart, Phys. Rev. Lett. **87**, 201806 (2001) [arXiv:hep-ph/0107002].
- [27] C. J. Monahan, H. Na, C. M. Bouchard, G. P. Lepage and J. Shigemitsu, Phys. Rev. D **95**, no.11, 114506 (2017) doi:10.1103/PhysRevD.95.114506 [arXiv:1703.09728 [hep-lat]].
- [28] E. McLean, C. T. H. Davies, J. Koponen and A. T. Lytle, Phys. Rev. D **101**, no.7, 074513 (2020) doi:10.1103/PhysRevD.101.074513 [arXiv:1906.00701 [hep-lat]].
- [29] S. Aoki *et al.* [Flavour Lattice Averaging Group], Eur. Phys. J. C **80**, no.2, 113 (2020) doi:10.1140/epjc/s10052-019-7354-7 [arXiv:1902.08191 [hep-lat]].
- [30] A. J. Buras, Nucl. Phys. B **434** (1995), 606-618 doi:10.1016/0550-3213(94)00482-T [arXiv:hep-ph/9409309 [hep-ph]].
- [31] A. J. Buras and L. Silvestrini, Nucl. Phys. B **548** (1999), 293-308 doi:10.1016/S0550-3213(99)00022-X [arXiv:hep-ph/9806278 [hep-ph]].
- [32] T. Huber, S. Kränkl and X. Q. Li, JHEP **09**, 112 (2016) doi:10.1007/JHEP09(2016)112 [arXiv:1606.02888 [hep-ph]].
- [33] M. Bordone, N. Gubernari, D. van Dyk and M. Jung, Eur. Phys. J. C **80** (2020) no.4, 347 doi:10.1140/epjc/s10052-020-7850-9 [arXiv:1912.09335 [hep-ph]].
- [34] A. Khodjamirian and A. V. Rusov, JHEP **08**, 112 (2017) doi:10.1007/JHEP08(2017)112 [arXiv:1703.04765 [hep-ph]].
- [35] G. Ricciardi, [arXiv:2103.06099 [hep-ph]].
- [36] D. Bigi and P. Gambino, Phys. Rev. D **94**, no.9, 094008 (2016) doi:10.1103/PhysRevD.94.094008 [arXiv:1606.08030 [hep-ph]].
- [37] R. H. Li, C. D. Lu, W. Wang and X. X. Wang, Phys. Rev. D **79**, 014013 (2009) doi:10.1103/PhysRevD.79.014013 [arXiv:0811.2648 [hep-ph]].
- [38] P. Colangelo, F. De Fazio, R. Ferrandes and T. N. Pham, Phys. Rev. D **73**, 115006 (2006) doi:10.1103/PhysRevD.73.115006 [arXiv:hep-ph/0604029 [hep-ph]].
- [39] W. F. Wang and Z. J. Xiao, Phys. Rev. D **86**, 114025 (2012) doi:10.1103/PhysRevD.86.114025 [arXiv:1207.0265 [hep-ph]].
- [40] G. Hiller, [arXiv:1804.02011 [hep-ph]].
- [41] S. Fajfer, SciPost Phys. Proc. **1** (2019), 010 doi:10.21468/SciPostPhysProc.1.010
- [42] F. U. Bernlochner, M. F. Sevilla, D. J. Robinson and G. Wormser, [arXiv:2101.08326 [hep-ex]].
- [43] J. Albrecht, D. van Dyk and C. Langenbruch, Prog. Part. Nucl. Phys. **120** (2021), 103885 doi:10.1016/j.pnpnp.2021.103885 [arXiv:2107.04822 [hep-ex]].

- [44] R. Fleischer, R. Jaarsma and G. Tetlalmatzi-Xolocotzi, Eur. Phys. J. C **81** (2021) no.7, 658 doi:10.1140/epjc/s10052-021-09419-8 [arXiv:2104.04023 [hep-ph]].
- [45] G. Banelli, R. Fleischer, R. Jaarsma and G. Tetlalmatzi-Xolocotzi, Eur. Phys. J. C **78** (2018) no.11, 911 doi:10.1140/epjc/s10052-018-6393-9 [arXiv:1809.09051 [hep-ph]].
- [46] J. L. Rosner, S. Stone and R. S. Van de Water, [arXiv:1509.02220 [hep-ph]].
- [47] R. Aaij *et al.* [LHCb], Phys. Rev. D **101** (2020) no.7, 072004 doi:10.1103/PhysRevD.101.072004 [arXiv:2001.03225 [hep-ex]].
- [48] I. Caprini, L. Lellouch and M. Neubert, Nucl. Phys. B **530** (1998), 153-181 doi:10.1016/S0550-3213(98)00350-2 [arXiv:hep-ph/9712417 [hep-ph]].
- [49] R. Fleischer, R. Jaarsma and K. K. Vos, Phys. Rev. D **94** (2016) no.11, 113014 doi:10.1103/PhysRevD.94.113014 [arXiv:1608.00901 [hep-ph]].
- [50] R. Aaij *et al.* [LHCb], Phys. Rev. Lett. **126** (2021) no.8, 081804 doi:10.1103/PhysRevLett.126.081804 [arXiv:2012.05143 [hep-ex]].
- [51] J. M. Flynn, T. Izubuchi, T. Kawanai, C. Lehner, A. Soni, R. S. Van de Water and O. Witzel, Phys. Rev. D **91**, no.7, 074510 (2015) doi:10.1103/PhysRevD.91.074510 [arXiv:1501.05373 [hep-lat]].
- [52] A. Bazavov *et al.* [Fermilab Lattice and MILC], Phys. Rev. D **100**, no.3, 034501 (2019) doi:10.1103/PhysRevD.100.034501 [arXiv:1901.02561 [hep-lat]].
- [53] I. Sentitemsu Imsong, A. Khodjamirian, T. Mannel and D. van Dyk, JHEP **02**, 126 (2015) doi:10.1007/JHEP02(2015)126 [arXiv:1409.7816 [hep-ph]].
- [54] J. Flynn, R. Hill, A. Jüttner, A. Soni, J. T. Tsang and O. Witzel, PoS **LATTICE2019**, 184 (2019) doi:10.22323/1.363.0184 [arXiv:1912.09946 [hep-lat]].